Government of **Western Australia**
Department of **Mines and Petroleum**

RECORD 2017/3

PROVENANCE, DEPOSITIONAL SETTING, AND REGIONAL CORRELATIONS OF THE ORDOVICIAN CARRANYA FORMATION, CANNING BASIN

by
LS Normore

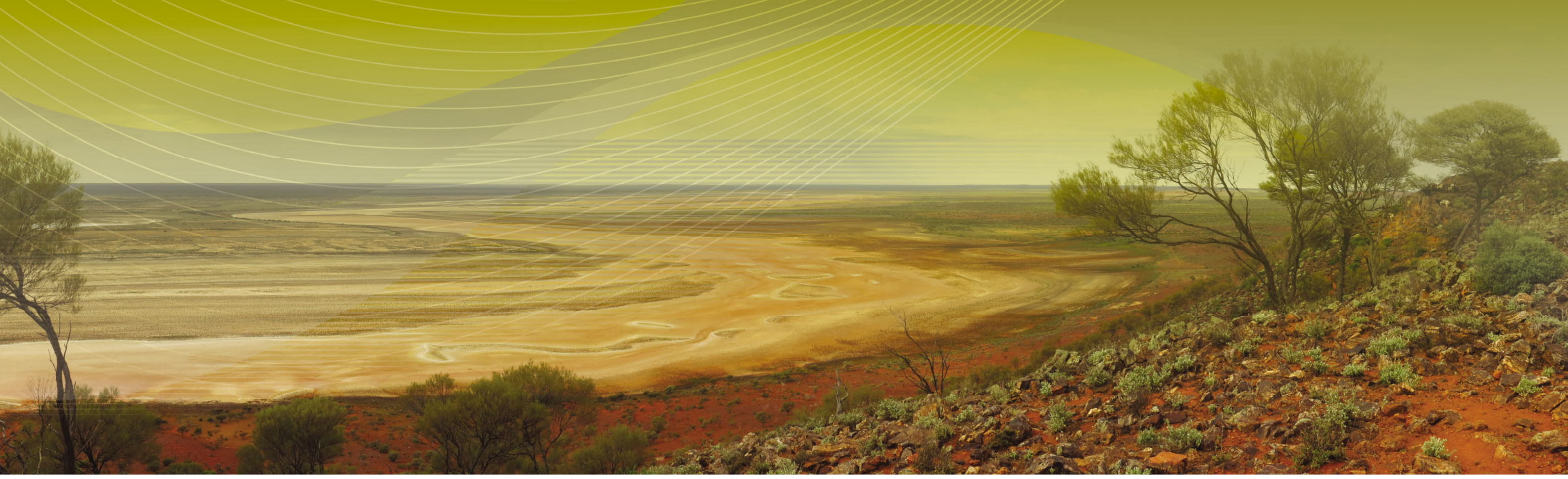

Geological Survey of
Western Australia

Government of **Western Australia**
Department of **Mines and Petroleum**

Record 2017/3

PROVENANCE, DEPOSITIONAL SETTING AND REGIONAL CORRELATIONS OF THE ORDOVICIAN CARRANYA FORMATION, CANNING BASIN

by
LS Normore

Perth 2017

Geological Survey of Western Australia

REFERENCE
The recommended reference for this publication is:
Normore, LS 2017, Provenance, depositional setting, and regional correlations of the Ordovician Carranya Formation, Canning Basin: Geological Survey of Western Australia, Record 2017/3, 22p.

National Library of Australia Card Number and ISBN 978-1-74168-717-0

Grid references in this publication refer to the Geocentric Datum of Australia 1994 (GDA94). Locations mentioned in the text are referenced using Map Grid Australia (MGA) coordinates, Zone 52. All locations are quoted to at least the nearest 100 m.

Published 2017 by Geological Survey of Western Australia
This Record is published in digital format (PDF) and is available online at <www.dmp.wa.gov.au/GSWApublications>.

Further details of geological products and maps produced by the Geological Survey of Western Australia are available from:
Information Centre
Department of Mines and Petroleum
100 Plain Street
EAST PERTH WESTERN AUSTRALIA 6004
Telephone: +61 8 9222 3459   Facsimile: +61 8 9222 3444
www.dmp.wa.gov.au/GSWApublications

Cover image: Elongate salt lake on the Yilgarn Craton — part of the Moore–Monger paleovalley — here viewed from the top of Wownaminya Hill, 20 km southeast of Yalgoo, Murchison Goldfields. Photograph taken by I Zibra for the Geological Survey of Western Australia

Contents

Figures

Provenance, depositional setting and regional correlations of the Ordovician Carranya Formation, Canning Basin

by

LS Normore

Abstract

The Carranya Formation is a sequence of oxidized Paleozoic sedimentary rocks that crop out on the northeastern extent of the Canning Basin in the Billiluna Shelf and Balgo Terrace areas. These siliciclastic rocks include fine- to medium-grained quartz sandstone, pebble conglomerate, and minor siltstone, previously assigned an Ordovician age, based on a single trilobite pygidium, originally identified as *Dikelokephalina* sp. These rocks have been correlated to the oldest sedimentary rocks of the subsurface Canning Basin, including the Kunian Sandstone of the Prices Creek Group, the Nambeet Formation, and the Wilson Cliffs Sandstone.

Formerly mapped outcrops were revisited to define the relationship of these sedimentary rocks with equivalent subsurface rocks as identified in petroleum wells. The Carranya Formation has been confirmed in five of the six previously identified outcrops. Three of the outcrops were logged in detail to identify any lateral sedimentological changes.

A variety of distinctive sedimentary and diagenetic structures along with macro and trace fossils were observed in the Carranya Formation. These features presented on detailed sedimentary logs have allowed subdivision of the formation into a lower tidal mudflats member and an upper tidal sandflats to fluvial member. The lower tidal member is developed locally at the Carranya Formation type section. Subsequent relative sea-level fall resulted in the deposition of the overlying, upper regressive fluvial member.

Paleocurrent measurements of the Carranya Formation indicate a sediment source to the northwest. Published provenance interpretations based on detrital zircon analysis suggest an original provenance to the southeast from the Arunta and Musgrave Orogens, to the southwest in the Paterson Orogen, and a much more distal source in East Antarctica. This could suggest a more regional Neoproterozoic cover had once been deposited across the North Australian Craton, sourced from the south and subsequently eroded.

A potential regional correlation of the Carranya and Goldwyer Formations is suggested based on detrital zircon evidence. The new correlation also has implications for reservoir potential along the eastern edge of the Canning Basin.

KEYWORDS: geochronology, hydrocarbons, ichnofossils, palaeocurrents, provenance, sedimentology, sedimentary environments, sedimentary structures, stratigraphy

Introduction

The Canning Basin is an asymmetric, northwest–southeast-trending sedimentary basin located in the northern part of Western Australia with an onshore surface area of over 530 000 km² and a sedimentary sequence over 10 km thick. It is bounded by the Kimberley region to the northeast, the Pilbara Craton to the southwest, and onlaps the Musgrave Province, Arunta Orogen, and the Amadeus, Murraba, and Birrindudu Basins on the eastern side. The basin is partially covered by the Gunbarrel Basin to the south and extends into the offshore to the west, where it is onlapped by Cenozoic sedimentary rocks of the Roebuck and Browse Basins of the North West Shelf (Fig. 1). This extensive basin has been divided into over twenty distinct structural elements (Fig. 1; Hocking, 1994). The primary structural components are two northwest–southeast-trending troughs separated by a central positive flower structure, and surrounded on the northern and southern margins by extensive shelf regions. Further subdivision of the basin is the result of a southwest–northeast-trending plateau, separating distinct sub-basins to the northwest and southeast (see Fig. 1 for names of Canning Basin subdivisions).

The Canning Basin onshore sedimentary rocks are predominantly of Paleozoic age, overlain by a thin Mesozoic and Cenozoic cover. This Record will focus on supersequence 'A' of the initial 'Ordovician–Silurian megasequence' of the Canning Basin (Kennard et al., 1994), which is dominated by a thick interval of Ordovician and Silurian siliciclastic and carbonate sedimentary rocks. This supersequence is identified in both subsurface and outcrop (Fig. 2).

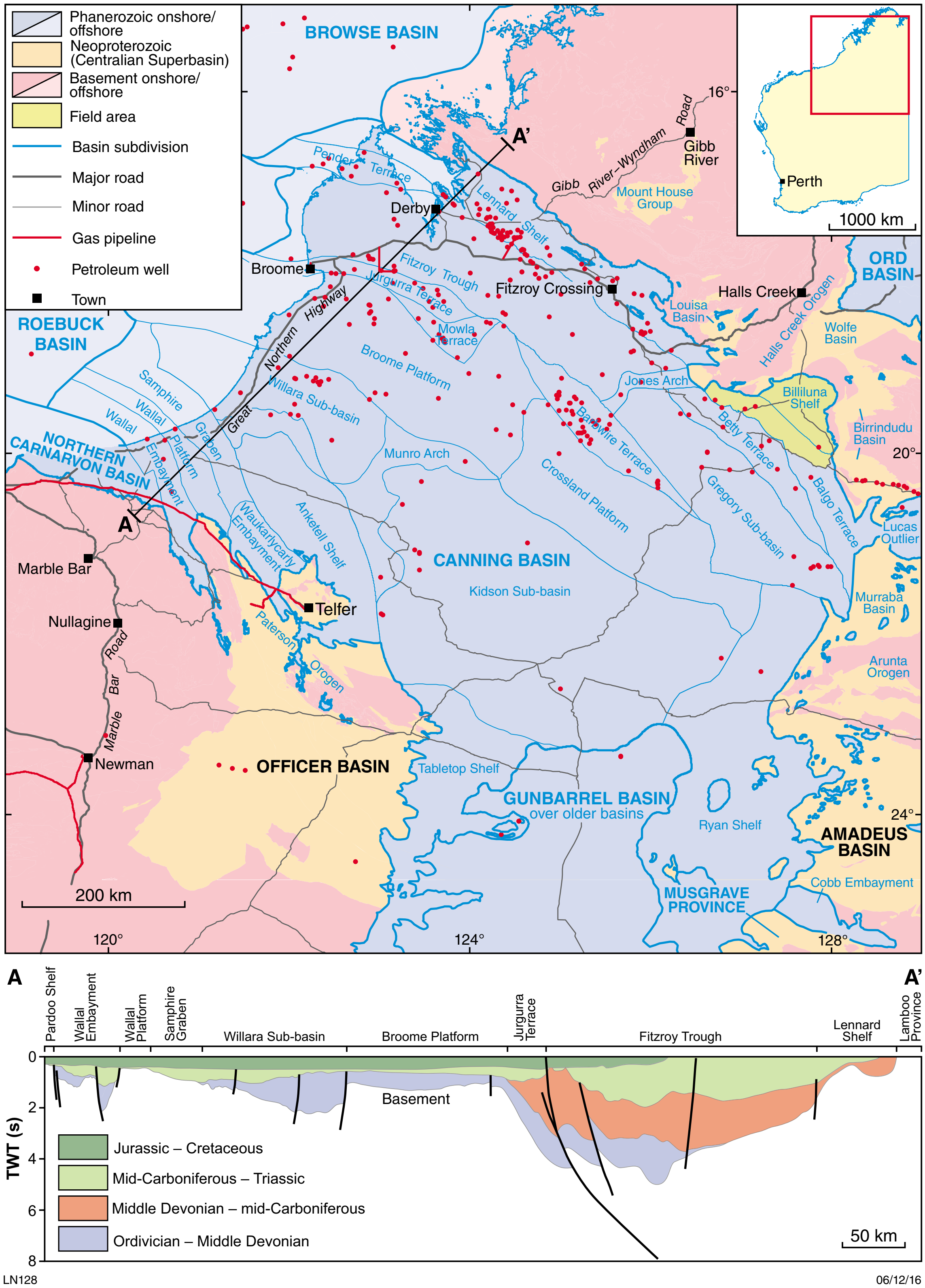

Figure 1. Principal structural elements of the Canning Basin (after Zhan, 2017)

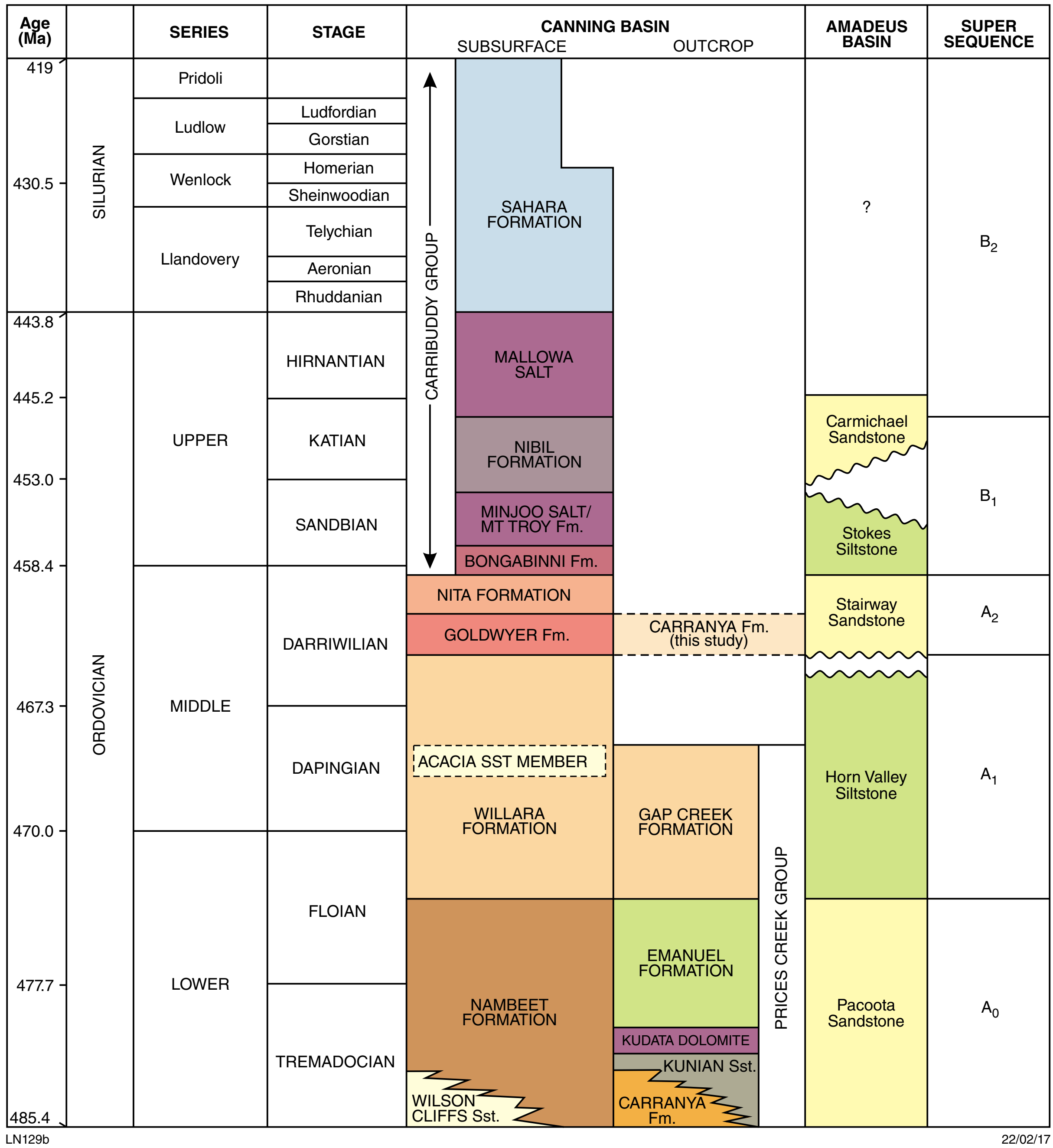

Figure 2. Nomenclature of Ordovician strata of the Canning Basin and Amadeus Basin. Stratigraphic subdivision of the Ordovician succession of the Canning Basin (modified from Haines, 2004 and Nicoll et al., 2013; supersequences from Kennard et al., 1994). Carranya Formation with alternate stratigraphic positions. Tremadocian correlation from Kennard et al., 1994 and Haines and Wingate, 2007a,b; Darriwilian from this study.

Subsurface nomenclature of supersequence 'A' from oldest to youngest comprises the Nambeet Formation, (laterally equivalent to the Wilson Cliffs Sandstone), followed by the Willara, Goldwyer, and Nita Formations as identified from numerous petroleum and mineral exploration wells throughout the Canning Basin (Fig. 2). Ordovician outcrops are found in three distinct parts of the basin. The first is the Prices Creek area on the southern edge of the Lennard Shelf (Fig. 3), where the stratigraphy of the Prices Creek Group has been defined and refined in various publications, e.g. Guppy and Orpik (1950) and Nicoll et al. (1993). The second outcrop area is along the northern edges of the Balgo Terrace and Billiluna Shelf (Fig. 3). These oxidized sandstones, pebble conglomerates, and minor siltstones were first called the Carranya Beds by McTavish (in Playford et al., 1975) and are now formally called the Carranya Formation (Cockbain and Hocking, 1989). A third area of Ordovician outcrop was recently discovered in the Cobb Embayment area in the southeast of the Canning Basin, next to the Musgrave Province (Haines et al., 2015).

This study revisited previously identified Carranya Formation outcrops to establish definitive links between outcrop and subsurface stratigraphy. The sedimentology, paleocurrent, and detrital zircon geochronolgy of the Carranya Formation were investigated in conjunction with macro and trace fossil assemblages to determine subsurface and outcrop correlations, the environment of deposition, petroleum potential, and to assist in regional correlations.

Previous work

A thick sequence of Phanerozoic sedimentary rocks was first mapped in the northern Canning Basin by the Bureau of Mineral Resources (now Geoscience Australia) during the period from 1948 to 1952 (Guppy et al., 1958). This geological mapping of the 'Fitzroy Basin', now divided into multiple basin components, was subsequently followed up in 1955 by continued mapping of Paleozoic and Mesozoic outcrops farther east on the Balgo Terrace

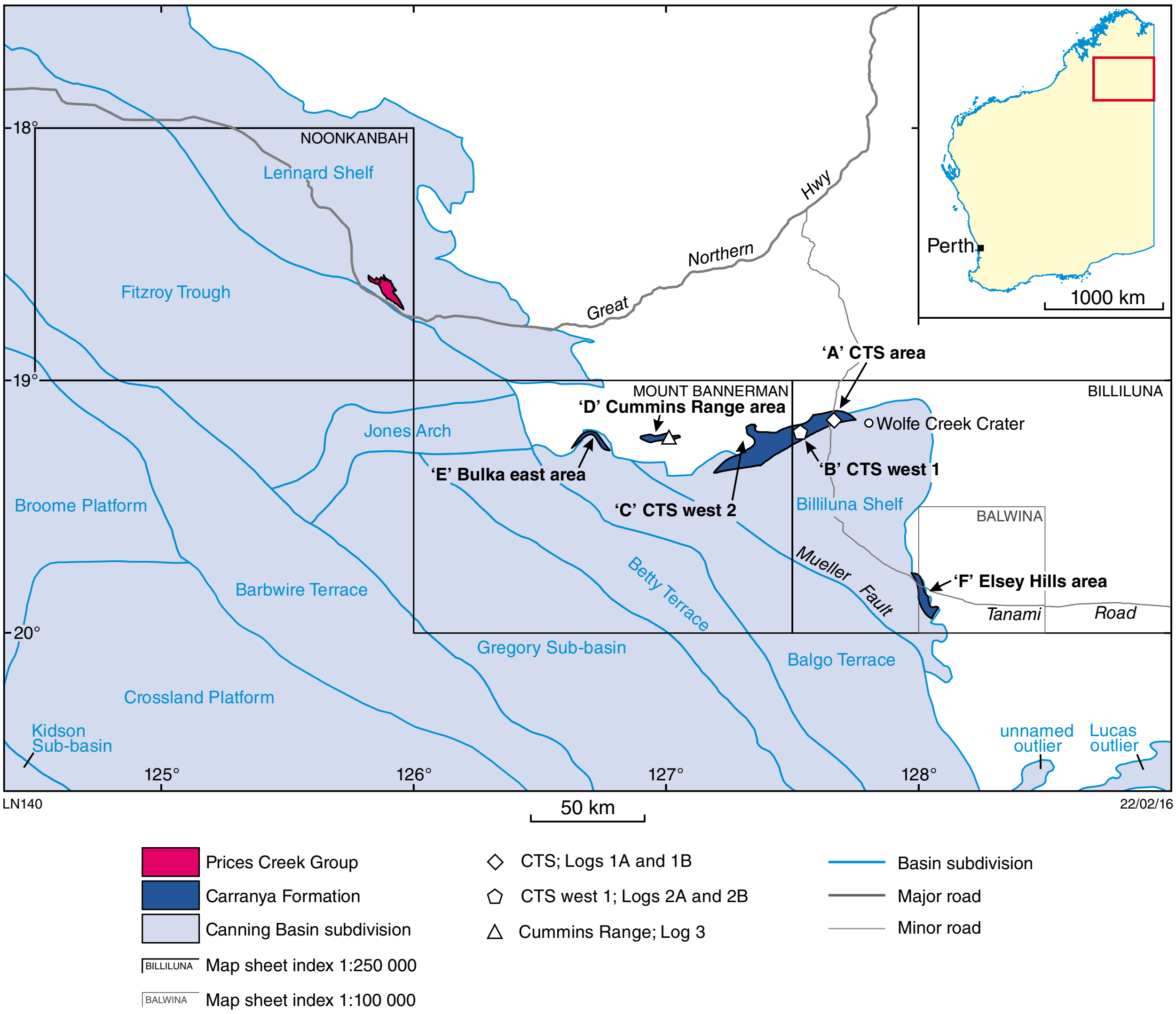

Figure 3. **Ordovician outcrop in the eastern Canning Basin with standard 1:250 000 map sheets superimposed. The Prices Creek Group is situated on the Noonkanbah 1:250 000 sheet and the Carranya Formation on the Mount Bannerman and Billiluna 1:250 000 sheets and the Balwina 1:100 000 sheet.**

and Billiluna Shelf (Veevers and Wells, 1961; Casey and Wells, 1964). This round of mapping defined the northeastern boundary of the Canning Basin, identifying several areas of Ordovician sedimentary rocks. An Ordovician age for these rocks was interpreted based on a single trilobite pygidium identified as *Dikelokephalina* sp. (Fig. 4; Gilbert-Tomlinson in Casey and Wells, 1964). A second edition mapping was completed in the 1970s, resulting in the BILLILUNA and MOUNT BANNERMAN (1:250 000) maps (Yeates and Muhling, 1977; Blake et al., 1977a). Recent mapping of the BALWINA (1:100 000) map also covered the eastern most extent of these Ordovician outcrops (Eacott et al., 2014).

The unnamed Ordovician sandstones, conglomerates, and siltstones identified at several localities on the BILLILUNA and MOUNT BANNERMAN (1:250 000) map sheet areas by these early studies would later be named the Carranya Formation (Playford et al., 1975; Blake et al., 1977a; Cockbain and Hocking, 1989). Previous 1:250 000 scale mapping identified six distinct areas of Carranya Formation outcrop (Fig. 3).

The Carranya Formation type section (CTS) is named after the Carranya Station where it is located 103 km south of the town of Halls Creek (MGA 358636E 7880883S). The type section was originally measured as being 150 m thick, and described as a sandstone and conglomeratic sedimentary interval with a fossiliferous sandy siltstone base (McTavish in Playford et al., 1975). Yeates and Muhling (1977) provide more detail on the Carranya Formation, describing it as a variegated (white, yellow, brown, and orange), thinly bedded to laminated, fine- to medium-grained sandstone with minor thin beds of rounded pebble to cobble conglomerate, and intraformational claystone clast conglomerate. Measured sections at the type section and 13 km to the west were originally logged as being 107 m and 135 m thick, respectively, both with an unexposed base and an eroded top. The Carranya Formation has been previously correlated with the lower unit of the Wilson Cliffs Sandstone and the Nambeet Formation (Kennard et al., 1994; Haines and Wingate, 2007b). It also has been correlated to the lower Emanuel Formation (Playford et al., 1975; McTavish and Legg, 1976), now renamed the Kunian Sandstone (Nicoll et al., 1993).

Carranya Formation: new field observations

Overview

A review of the location and topography of Carranya Formation outcrops in the Canning Basin from new field observations is presented below, along with a description of a variety of observed geological attributes, including contact relationships, lithology, petrography, paleocurrent data, sedimentary, and diagenetic structures and fossil assemblages. These characteristics are used to help define the depositional environment and provenance of the Carranya Formation. Final discussions provide correlation to the more extensively studied subsurface sedimentary units of the Canning Basin, potential regional correlations to adjacent sedimentary basins, and implications for hydrocarbon prospectivity.

Location and topography

The Carranya Formation crops out on the outer edge of the Billiluna Shelf on the limbs of a broad synclinal structure, plunging shallowly to the southwest (Fig. 5). Field work by the Geological Survey of Western Australia (GSWA) in June 2014 covered five of the six previously mapped Carranya Formation outcrop areas (Fig. 5). Three areas are exposed in the BILLILUNA 1:250 000 map sheet area (Blake et al., 1977b) and three in the MOUNT BANNERMAN 1: 250 000 map sheet area (Yeates et al., 1978). Five of the outcrop areas are present on the northern limb of the syncline (Fig. 5; Locations A, B, C, D, and E) with only the Elsey Hills location on the southern limb (Fig. 5; Location F). The northern limb outcrops are offset by either parasitic folding related to the main syncline or left lateral faulting.

The type section for the Carranya Formation is obliquely crossed by the Tanami Road, 14 km west of the Wolfe Creek Meteorite Crater (Fig 5; Location A). Outcrop is best observed on a slight topographical rise east of the track with further outcrops to the west.

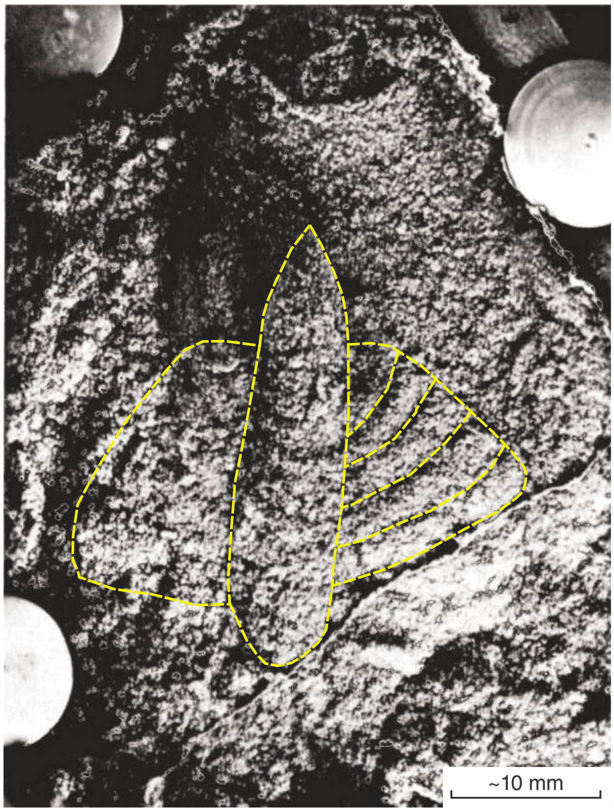

Figure 4. The only potentially age-diagnostic fossil found from the Carranya Formation. Originally identified as *Dikelokephalina* sp., this provides the Ordovician age (after Casey and Wells, 1964); thumbtack head 10 mm.

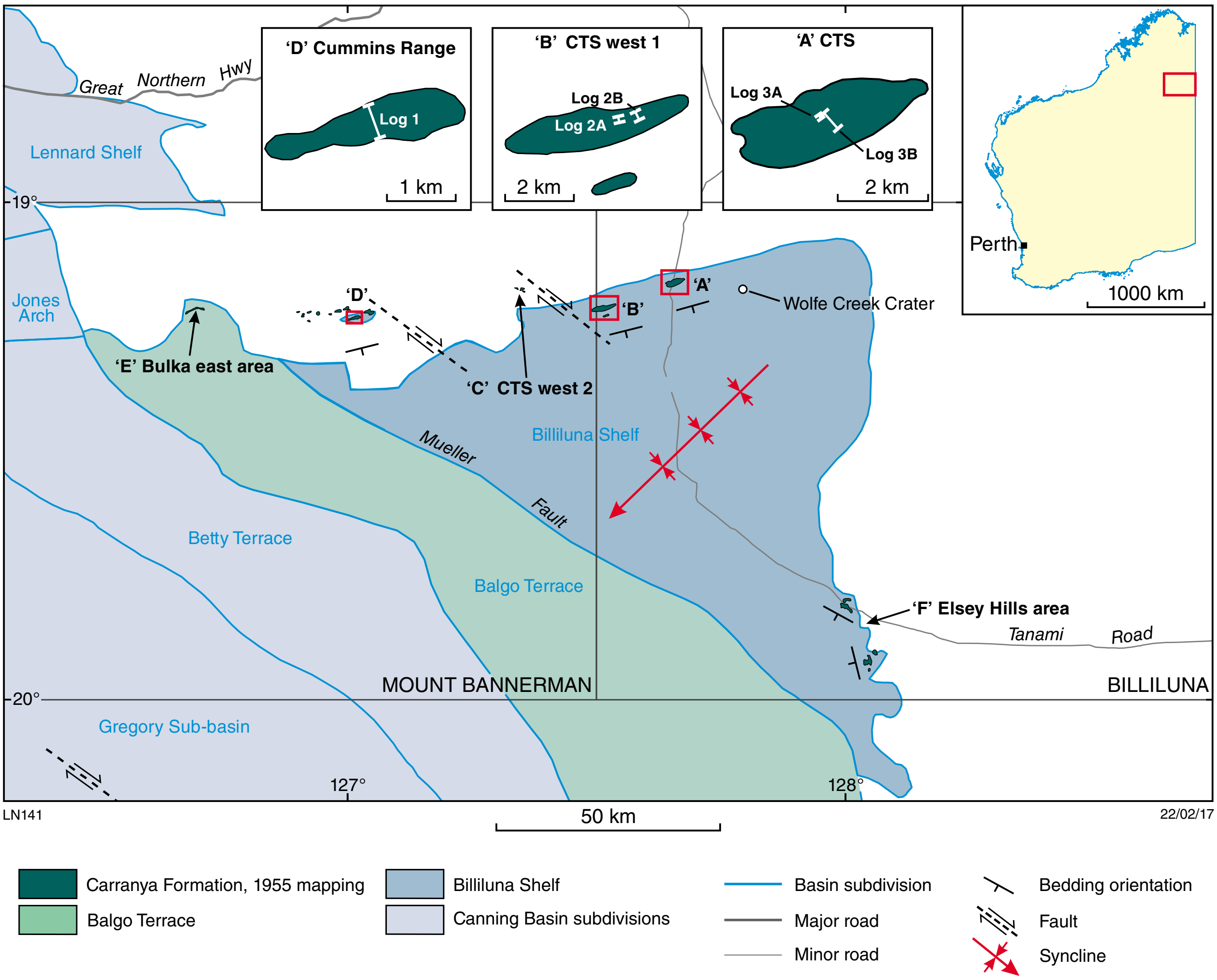

Figure 5. **Carranya Formation outcrop in the study area with structural interpretation and location of stratigraphic logs: 'A' CTS, 'B' CTS west 1, 'C' CTS west 2 (not visited), 'D' Cummins Range, 'E' Bulka east, and 'F' Elsey Hills. Insets correspond to red boxes on the main map.**

CTS west 1 (Fig. 5; Location B) is located 15 km west-southwest, along strike of the type section near the boundary of the MOUNT BANNERMAN map sheet. This locality is partially covered by regolith, but is present on a more pronounced east–west-trending ridge.

CTS west 2 (Fig. 5; Location C) was not visited due to difficult vehicle access and is located a further 18 km to the west-northwest in the northeastern corner of the MOUNT BANNERMAN 1:250 000 map sheet area. Continuing along strike to the west-southwest for another 35 km is the Cummins Range (Fig. 5; Location D). Several outcrops of Carranya Formation were previously mapped in the Cummins Range area (Yeates et al., 1978), but most outcrops in the range were identified as older basement sedimentary rocks. Only one outcrop of the Carranya Formation was confirmed during this fieldwork. This locality is found on a plateau on the southern edge of the range with more extensive Proterozoic hills occupying the majority of the range. It consisted of a 30 m-high asymmetric ridge, dipping 15–20º to the south (Fig. 6 a).

The westernmost outcrop of the Carranya Formation visited during this study was in the Bulka east area (Fig. 5; Location E), where the topography was most pronounced with a 50 m-high sharp ridge (Fig. 6b). The final area was located on the southern limb of the Billiluna Shelf syncline in the Elsey Hills area (Fig. 5; Location F) with low rubbly, 20 m-high hills (Fig. 6c).

Contacts

The Elsey Hills area (Fig. 5; Location F) is the only location where the basal contact of the Carranya Formation is exposed. The base appears to unconformably overlie Proterozoic basement originally mapped as the Baines Beds (Blake et al., 1977b), but recently mapped as the undivided Birrindudu Group on the BALWINA 1:100 000 map sheet (Eacott et al., 2014). A conglomerate interval with subrounded to subangular pebbles and cobbles, made up of the underlying orthoquartzite, overlies the erosional contact of the Carranya Formation basement (Fig. 7a). This contact is also offset due to faulting in the area.

Figure 6. Outcrop views of the Carranya Formation: a) southern Cummins Range; looking east, beds dipping to the southeast; car toward the left side of image for scale (circled) (MGA 290920E 7872238N); b) Bulka east outcrop profile; looking southeast, beds dipping southeast; ridge 50 m high; (MGA 258247E 7873878N); c) oblique view along Elsey Hills outcrop; looking southeast, beds dipping west-southwest; geology hammer in left foreground for scale (circled), 10 cm increments (MGA 396095E 7808156N)

The Bulka east area (Fig. 5; Location E) provides the only upper contact of the Carranya Formation. At this location, a well-exposed unconformable contact is observed with a thick, poorly sorted, imbricated, boulder conglomerate, eroding into the underlying sedimentary rocks (Fig. 7b). This overlying conglomerate has previously been mapped as the Permian Grant Formation (Yeates et al., 1975; Yeates and Muhling, 1977), later revised and renamed Grant Group (Crowe and Towner, 1976).

Lithology and sedimentary structures

The Carranya Formation is a siliciclastic succession of sedimentary rocks consisting mainly of sandstone with minor conglomerate and rare siltstone. The sandstone is a fine- to medium-grained quartz arenite (Fig. 8a) with colours ranging from white to pink to light orange. It weathers orange-brown, due to precipitation of iron oxide as thin rinds over quartz grains during weathering (see section on *Petrography*). The sandstone is generally thin to medium bedded, but occasionally thick beds are found where conglomerate units grade up into sandstone.

Conglomerate interbeds are present throughout the Carranya Formation, but are more common in the lower half of the section, decreasing in thickness and number up-section, eventually transitioning to normally graded pebbly sandstone (Fig. 8b). Conglomerate beds contain quartzite pebbles to cobbles, which generally form a clast-supported lag at the base of the bed (Fig. 8c).

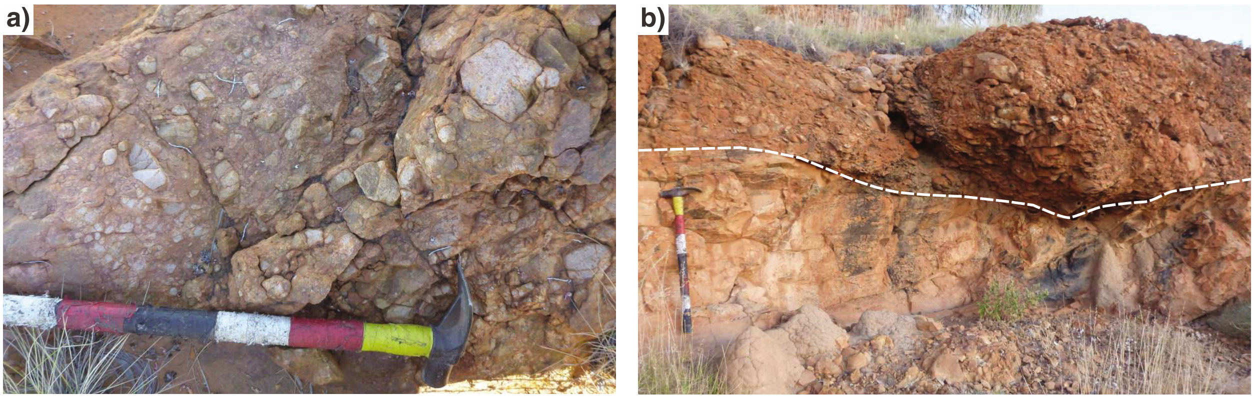

LN132 05/05/16

Figure 7. Carranya Formation stratigraphic contacts: a) base of the Carranya Formation immediately above unconformity/ faulted contact with basement; Elsey Hills locality; poorly sorted, subrounded to angular, pebble- to cobble-sized quartzite clasts in an orange-pink sandstone matrix; (MGA 401838E 7798479N); b) unconformable contact between Carranya Formation and overlying Permian Grant Group; Bulka east locality; erosional surface of poorly sorted, clast-supported, imbricated cobble- to boulder-sized conglomerate overlying an erosional surface cutting into thin- to medium-bedded Carranya Formation sandstone (MGA 258107E 7873899N). Geology hammer for scale; in both images with 10 cm increments marked on handle.

Clasts are commonly well rounded and poorly sorted, displaying a fining-upward trend, but no distinct imbrication. Conglomerate matrices are composed of the same fine- to medium-grained quartz arenite as the interbedded sandstone.

A thin siltstone to very fine-grained sandstone interval is found near the base of the section. This interval was only identified at the type section and Bulka east areas and contains macrofossils and strong bioturbation (see section on *Bioturbation and macrofossils*).

While the type section area is composed of all three lithologies, CTS west 1, Cummins Range, and Elsey Hills are primarily sandstone with conglomerate interbeds. The sedimentary rocks observed at the Bulka east location (Fig. 5; Location E) vary slightly from all other Carranya Formation outcrops. Sandstones are tan to orange-brown, thin to medium bedded, and fine grained with minor lithic fragments and feldspar grains. These sandstones also have rare interbeds of purple, thin wavy, laminated siltstone.

Sedimentary structures provide an understanding of how a sedimentary rock was deposited while diagenetic structures indicate processes acting on the rocks after burial. Sedimentary structures used to indicate paleocurrents are discussed in the paleocurrent analysis section below. Additional sedimentary structures preserved at the CTS and CTS west 1 include angular to tabular intraformational siltstone rip-up clasts (Fig. 8e) and slumped bedding (Fig. 8f). While the lithology is similar to the CTS, sedimentary structures in the Elsey Hills area are restricted to trough cross-bedding and pebble to cobble lag deposits in fining-upward sequences. Erosive sandstone channels (Fig. 8a) and large-scale, planar cross-bedding were prominent on the main cliff section at Cummins Range.

Diagenetic structures include liesegang banding (Fig. 8g) and carbonate-cemented concretions (Fig. 8h). Liesegang bands were found at the CTS, CTS west 1 and Bulka east, radiating perpendicular to bedding, while concretions were found at the CTS and CTS west 1.

Figure 8. (opposite) Field photographs of the Carranya Formation: a) orange-brown, thin- to medium-bedded, fine- to medium-grained, quartz arenite with stacked channelized sandstone beds; dashed white line at the base of sandstone channel; 10 cm increments on geology hammer; Cummins Range (MGA 291165E 7872329N); b) well-rounded, clast-supported quartzite pebble lag located at the base of a channel deposit; Elsey Range (MGA 396270E 7807918N); c) normally graded beds of conglomerates, pebbly sandstone, and sandstone; CTS (MGA 358454E 7880718N); d) orange-brown, thin- to medium-bedded sandstone interbedded with dark brown siltstone; CTS (MGA 358525E 7880771N); e) tabular to elongate, slightly deformed, angular siltstone rip-up clasts in a sandstone matrix; scale bar in cm; CTS (MGA 358525E 7880771N); f) distorted and slumped bedding in medium-grained sandstone; 10 cm increments on geology hammer; CTS (MGA 358803E 7880859N); g) liesegang banding perpendicular to bedding; scale bar in cm; CTS (MGA 358957E 7880698N); h) cobble-sized, carbonate-cemented concretion, slightly flattened due to compaction, suggesting early diagenesis; CTS (MGA 358630E 7880852N)

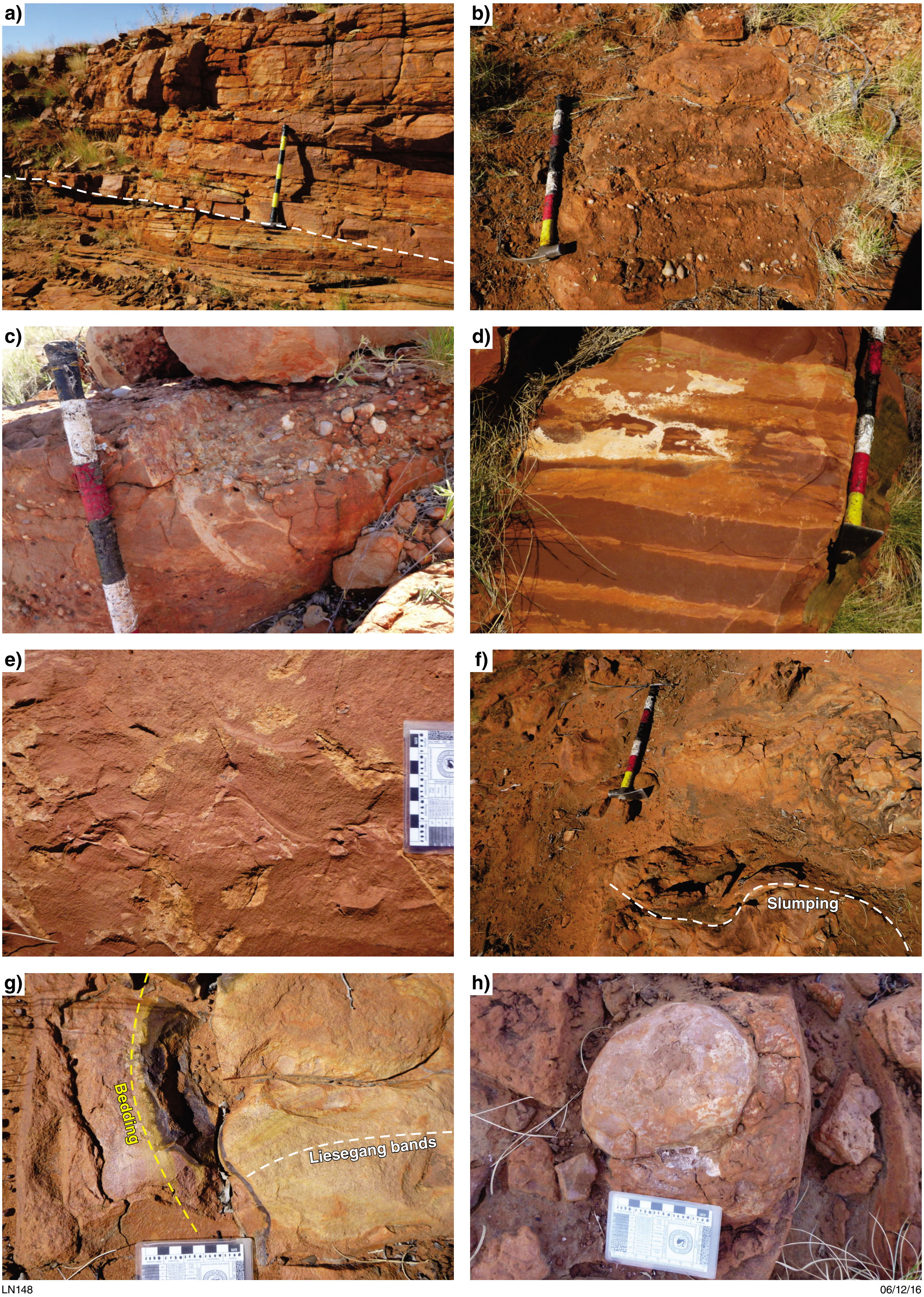
a)
b)
c)
d)
e)
f)
Slumping
g)
Bedding
Liesegang bands
h)
LN148
06/12/16

Paleocurrent analysis

Paleocurrent analysis provides direct information regarding the orientation of sedimentary systems, the provenance of sediment supply and can aid in determining depositional settings. A variety of paleocurrent indicators have been used to determine the general paleoflow direction during deposition of the Carranya Formation (Fig. 9). These indicators can be subdivided into three types of sedimentary structures: cross-bedding (Fig. 9a–c), ripples (Fig. 9d–f) and current lineations (Fig. 9g,h). Twenty-three paleocurrent measurements were recorded from outcrop. Paleocurrents were restored to horizontal bedding, using Wulff stereonets before plotting on rose diagrams (Fig. 10).

The CTS area had six measurements of paleocurrent, indicating a bidirectional flow to the west-northwest and southeast (Fig. 10a). Paleocurrent directions were taken from trough cross-bedding (Fig. 9a), flat-topped asymmetric ripples (Fig. 9f), and current lineations with accompanying current crescents (Fig. 9g). Sharp-crested asymmetric ripples were also found at CTS (Fig. 9d), but could not be used for paleocurrent measurements as they were only observed in float.

The CTS west 1 area had seven paleocurrent measurements with the main flow direction to the south-southeast and a minor component to the northwest (Fig. 10b). Measurements were taken from trough cross-bedding, current lineations (Fig. 9h), and small-scale, steeply dipping, sigmoidal cross-bedding (Fig. 9c). The Elsey Hills area had the most diverse paleocurrents to the northwest, northeast, and southeast (Fig. 10c). All paleocurrents from this location were measured from trough cross-bedding. The final location where paleocurrents were recorded was the Cummins Range. Measurements were taken from planar cross-bedding based on foreset dip direction (Fig. 9b) and from round-crested, asymmetric ripples (Fig. 9e). Paleocurrents at Cummins Range flowed mainly to the south-southeast and east-northeast with a minor component to the north-northwest (Fig. 9d).

A combined dominant flow for all measurements had a mean paleocurrent direction from east to south with a minor bidirectional flow to the northwest. The variability in paleocurrent direction was best demonstrated at the Cummins Range locality, where asymmetric ripples on adjacent bedding planes ranged from northwest to northeast.

Sedimentary logs

Five sedimentary logs were measured through the Carranya Formation: two at both CTS and CTS west 1, and one at the Cummins Range (Fig. 11). All logs were measured over sporadic outcrop with true thickness calculated from GPS locations and the dip of bedding. The thickest section measured was 196 m at the CTS (Fig. 11, Log 3B; Fig. 5, Location A) dominated by fine- to medium-grained sandstones, interbedded with pebbly sandstone and subordinate pebble to cobble conglomerate. A second log was measured 100 m to the west of Log 3B. It records the fine-grained, bioturbated, and fossiliferous interval found at the base of the type section (Fig. 11, Log 3A). This fossiliferous zone is not laterally continuous due to truncation to the east by conglomeratic channel deposits that have eroded down into the finer grained fauna-rich succession. No upper or lower contacts to the formation were observed at the type section location. Previous estimates have suggested 500 m for the Carranya Formation (Yeates et al., 1975).

Two measured sections were taken 500 m apart at CTS west 1 (Fig. 11, Logs 2A and 2B; Fig. 5, Location B) to identify lateral facies changes across the Carranya Formation. The sections were 150 m and 135 m thick with similar lithologies to the type section. Although the outcrop is discontinuous, a lack of continuity of specific conglomerate beds is apparent between logs. The width of conglomerate-filled channels is difficult to determine due to the intermittent nature of the outcrop. No upper or lower contacts to the formation were observed at CTS west 1, but the base of the outcrop is inferred to be close to the lower contact because of the presence of quartzite boulders in float.

One hundred and sixty metres of Carranya Formation were measured at Cummins Range (Fig. 11, Log 1; Fig. 5, Location D). While this was the most continuous exposure of outcrop from the Carranya Formation, fossils and contact relationships were not observed. No log was taken at Elsey Hills, but the Carranya Formation is estimated to be 150 m thick at this locality.

Figure 9. (opposite) Sedimentary structures providing paleocurrent data for the Carranya Formation: a) trough cross-bedding; geology hammer pointing down at the centre of a trough; paleocurrent flow direction away from viewer to the southeast; 10 cm increments on geology hammer; CTS (MGA 358842E 7880796N); b) sharp erosive contact of fluvial channel cutting into large-scale, cross-stratified, thickly bedded, medium-grained sandstone; paleocurrent to the left; Cummins Range, (see also Fig. 8a for stacked channels), (MGA 290920E 7872239N); c) cross-bedded, medium-grained sandstone with tabular cross-bedding, having curved top and bottom-sets; flow to the left; scale bar in cm, CTS west (MGA 345008E 7875193N); d) asymmetric bifurcating current ripples with a wavelength of 40 mm and amplitude of 5 mm; paleocurrent towards bottom of photo; CTS (MGA 358525E 7880771N); e) round-crested, slightly asymmetric ripples with a wavelength of 30 mm and amplitude of 4 mm, paleocurrent towards bottom-left of photo, Cummins Range (MGA 291169E 7872172N); f) flat-topped, asymmetric ripples with wavelength of 50 mm and height of 3 mm, paleocurrent to the left of photo, CTS (MGA 357792E 7880291N); g) current lineations, paleocurrent to the bottom right of photo; CTS (MGA 357792E 7880291N); h) current lineations, paleocurrent to the bottom right of photo, CTS west 1 (MGA 343887E 7875039N)

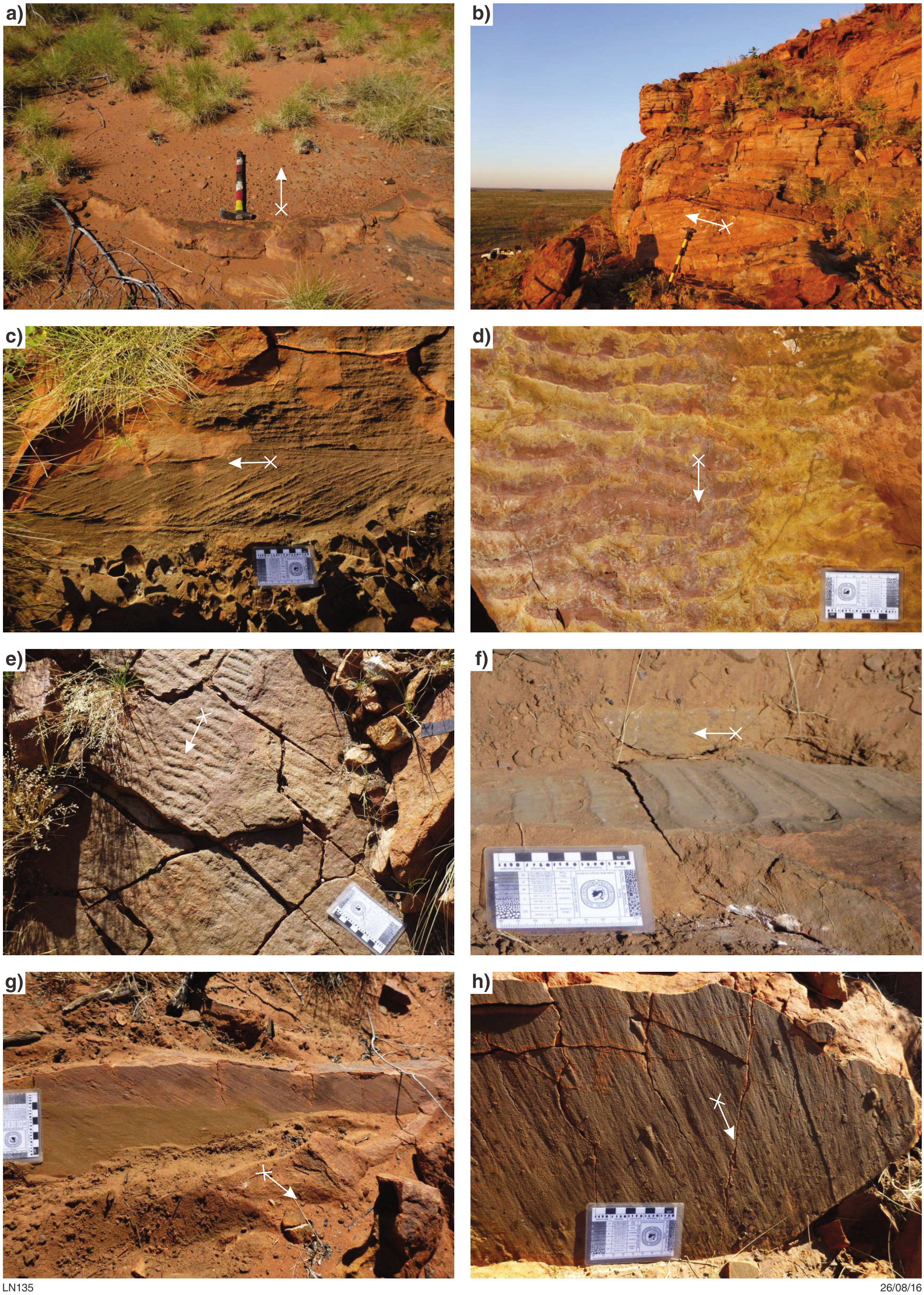
a)
b)
c)
d)
e)
f)
g)
h)
LN135
26/08/16

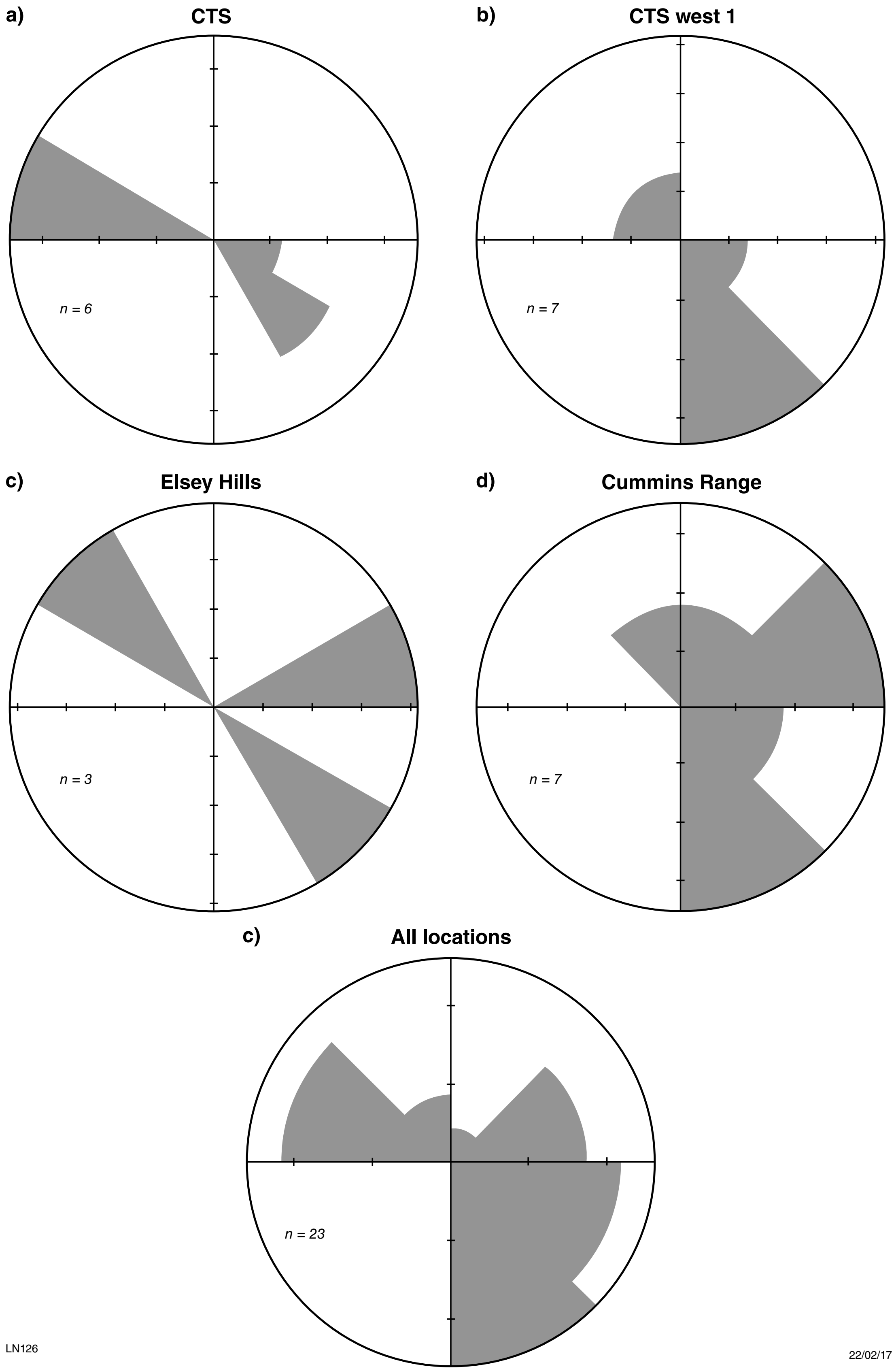

Figure 10. Rose diagrams presenting paleocurrent data from the Carranya Formation: a) CTS; bidirectional flow directions west-northwest and east-southeast; b) CTS west 1; predominantly to the southeast with minor component to the northeast; c) Elsey Hills; variable flow directions northwest, east, and southeast; d) Cummins Range; dominant paleocurrents to the south-southeast and east-northeast; e) all locations combined; dominant paleocurrent flow direction to the southeast, but minor components to northwest and northeast

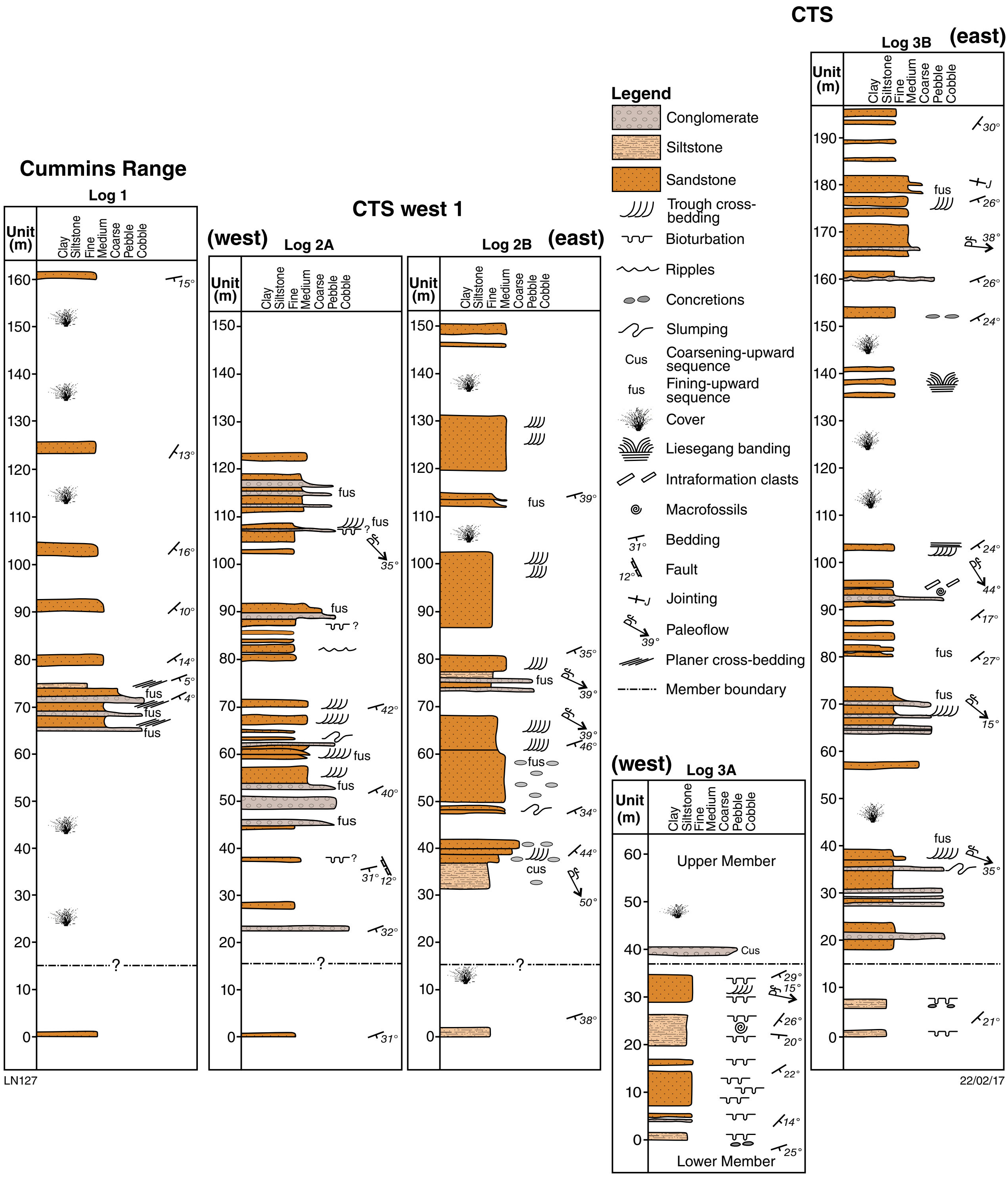

Figure 11. Stratigraphic logs for the Carranya Formation: Log 1 (base: MGA 291308E 7871989N, top: MGA 291131E 7872474N) from Cummins Range. Log 2A (base: MGA 344425E 7875261N, top: MGA 344470E 7875066N) and Log 2B (base: MGA 344907E 7875403N, top: MGA 345008E 7875193N) from CTS west 1. Log 3A (base: MGA 358648E 7880892N, top: MGA 358692E 7880800N) and Log 3B (base: MGA 358745E 7880931N, top: MGA 359038E 7880585N) from CTS

Bioturbation and macrofossils

The Carranya Formation preserves a diverse trace fossil assemblage, mainly produced by deposit-feeding organisms with rare suspension feeders. Bioturbation is primarily confined to the lower 35 m-thick siltstone and very fine-grained sandstone interval at the CTS (best seen in Fig. 11, Log 3A). Rare bioturbated beds are also observed at CTS west 1 (Fig. 11, Log 2A) and Bulka east. Bioturbation, when present, ranges from individual trace fossils to intervals where extreme bioturbation has completely removed the original sedimentary fabric.

Horizontal to subhorizontal, deposit-feeding burrows dominate trace fossil assemblages in the Carranya Formation. Examples of *Planolites* sp. (Nicholson, 1872) are straight to gently curved, cylindrical, and non-branching. They crosscut horizontal traces and range from 3–5 mm in diameter (Fig. 12a). Thicker, irregularly shaped, subhorizontal, branching burrows, up to 3 cm wide, resemble *Thalassinoides* sp. (Ehrenberg, 1938) (Fig. 12b). The feeding trace *Chondrites intracatus* (Brongniart, 1828; Seilacher, 2007) was observed at the Bulka east area (Fig. 12c) and also at the CTS (Fig. 12d). This delicate branching burrow system has a main vertical shaft to the surface from which dendritic burrows extend outward from 45 degrees to near horizontal. Only one suspension-feeding burrow was observed in the Carranya Formation. A distinctive example of *Arencolites* sp. (Salter, 1857) (Fig. 14e) was located at the CTS. It is an open U-shaped burrow, 12 cm from entrance to exit and with a central diameter of 3 mm, increasing to 6 mm at the ends. Multiple trace fossils have been observed on a single bedding plane (Fig. 12f).

Macrofossil molds are present in two main horizons at the CTS. The richest interval is located from 19–26 m on Log 3A (Fig. 11) and minor occurrences at 95 m on Log 3B (Fig. 11). The main fossil molds are of gastropods (Fig. 12g), but grain size and composition of the sandstone prevent detailed preservation and positive identification. However, gastropods have been previously identified as *Ophileta* (Legg in Playford et al., 1975). The gastropods of the Carranya Formation have been compared to those found in the Kunian Sandstone (Nicoll et al., 1993). Other macrofossils include rare brachiopods (Fig.12h), trilobite fragments (Fig. 4), and larger unidentifiable shell molds.

Enigmatic structures

Several structures were observed in the Carranya Formation that are difficult to reconcile as biogenic, sedimentary, or diagenetic structures and may be examples of microbial activity or previously undescribed trace fossils. Features reminiscent of *Kinneyia* wrinkle structures (Walcott, 1914; Hagadorn and Bottjer, 1997; Seilacher, 2007; Porada and Bouougri, 2007) are found at both the Elsey Hills and CTS west 1 locations (Fig. 13a). These features have been described as synsedimentary structures that form through gas entrapment under a thin microbial mat (Seilacher, 2007) and typically appear in inter- to subtidal depositional environments (Hagadorn and Bottjer, 1997). These features have also been known as 'peanut blisters' and are spherical, negative epireliefs up to 5 mm in diameter, and 1–2 mm deep. They are found on planar surfaces and can also be mistaken for raindrop impressions. A recent publication by Davies et al. (2016) also suggests an abiotic origin is possible for *Kinneyia* through accretion of wind-blown sand as adhesion structures in very shallow standing water.

Another puzzling feature found at the Elsey Hills location was a circular structure 25 mm in diameter (Fig. 13b). This structure has a 3 mm-wide concave impression on the outer edge with a central area of equivalent height as the surrounding bedding plane. It also has three distinctive radial ridges, less than 1 mm thick, joining the outer edge to the central convex portion of the impression. Two plausible explanations are proposed for the formation of this structure. The first explanation is a gas escape or dewatering structures similar to *Astropolithon* (Pickerill and Harris, 1979; Seilacher, 2007), which are sand volcanos covered by microbial mats that were exposed to some source of vibration. The second possibility is a coelenterate resting trace similar to *Bergauria* (Alpert, 1973).

Petrography

Two thin sections were cut from samples collected by Peter Haines (GSWA) at the CTS area during fieldwork in 2005 (MGA 358267E 7880557S; GSWA 184269, Wingate, 2007b). General composition, grain-size distribution, and texture indicate a mature to super-mature quartz arenite altered by the effects of diagenesis and weathering.

Figure 12. (opposite) Trace and macrofossils of the Carranya Formation: a) straight to slightly sinuous, horizontal *Planolites* trace fossils, 5mm wide and over 10 cm long; CTS (MGA 358630E 7880852N); b) irregularly shaped to bulbous *Thalassinodies*, 20–30 mm diameter and up to 10 cm long; CTS (MGA 358627E 7880861N); c) *C. intractus* feeding trace, main central vertical shaft with subhorizontal borrows, burrows less than 1 mm diameter, Bulka east locality (MGA 258107E 7873899N, GSWA sample 195479); d) planar surface of *C. intractus*; CTS (MGA 358627E 7880861N); e) *Arenicolites* dwelling trace 12 cm from entrance to exit of trace, burrow diameter 3 mm, widening to 6 mm at ends; CTS (MGA 358614E 7880836N; GSWA sample 195476); f) mixed trace fossil assemblage on same bedding plane; CTS (MGA 358727E 7880905N); g) stacked gastropod molds; CTS (MGA 358627E 7880861N, GSWA sample 195470); h) Brachiopod mold (yellow arrow); CTS (MGA 358700E 7880900N, GSWA sample 135997)

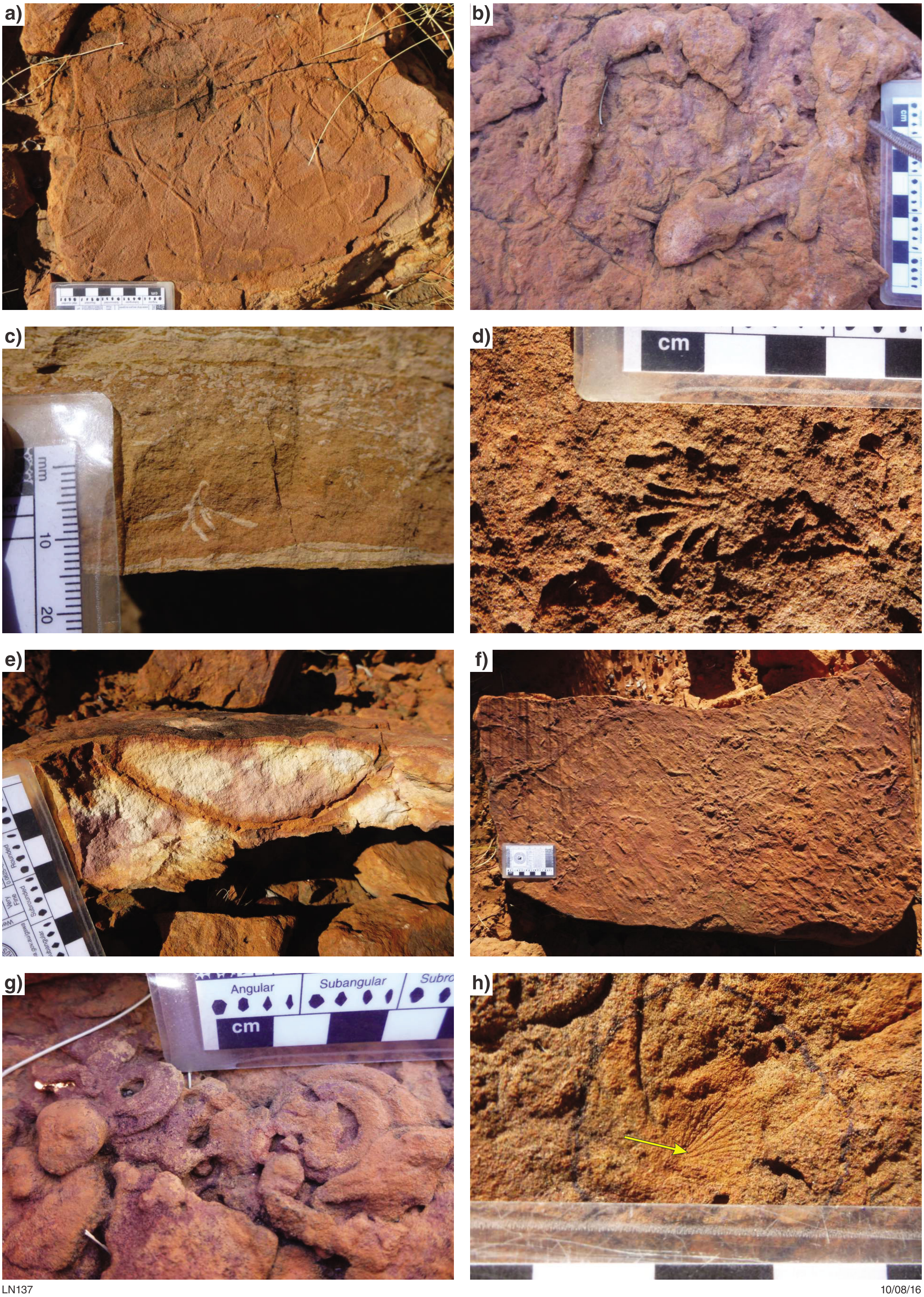
a)
b)
cm
c)
mm
10
20
d)
cm
e)
f)
g)
Angular
Subangular
cm
h)
LN137
10/08/16

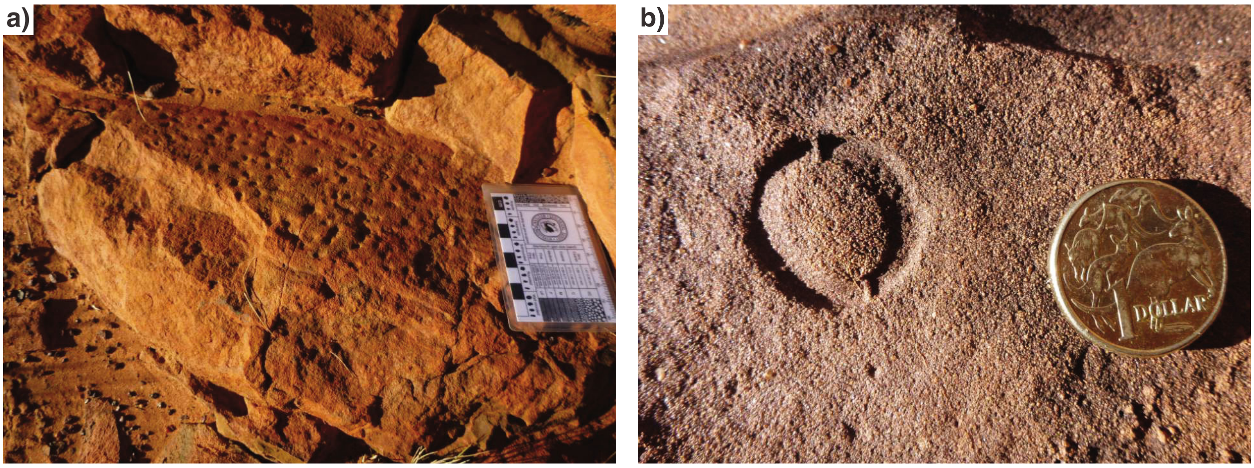

LN138 05/05/16

Figure 13. Enigmatic structures of the Carranya Formation: a) 'Kinneyia' wrinkle structures produced either from gas escape into a thin microbial film or adhesion structures from wind-blown sand into standing water; CTS west 1 (MGA 344469E 7875094N); b) circular impression 26 mm in diameter with two prominent radial ridges (a third, less conspicuous in left-lower section of structure) less than 1 mm thick connected to a raised central ring; coin 25 mm in diameter; Elsey Hills (MGA 396046E 7808111N, GSWA sample 195469)

Thin-section analysis reveals predominantly monocrystalline quartz grains with 5–10% opaque minerals and rare siltstone clasts (Fig. 14a). Opaque minerals consist of iron oxide coatings on quartz grain boundaries and unidentified infill of open pore space (Fig. 14b). Quartz grains are moderately to very well sorted, ranging from fine- to medium-sized grains. The texture of grains in the Carranya Formation generally ranges from moderate to well rounded, with occasional subangular to angular grains.

Textural maturity is biased by a number of factors taking place during diagenesis, primarily compaction of quartz grains during burial and quartz dissolution at grain-to-grain boundaries (Fig. 14b). Other factors changing the sphericity of quartz grains are the precipitation of authigenic quartz overgrowths, producing sharp crystal edges on some quartz grains (Fig. 14c). The combined effects of compaction and quartz cementation not only reduce the apparent textural maturity by increasing the angularity of grains, but also occlude the majority of the intergranular porosity.

Discussion

Depositional environment

A shallow-marine and shoreline depositional environment was first proposed for the Carranya Formation by Yeates et al. (1975). Based on fossils and sedimentary structures, an intertidal sandflat depositional environment has also been suggested (McTavish and Legg, 1976). The present study combined contacts, lithology, sedimentary structures, bioturbation, paleocurrents, and petrography to provide a more detailed account of the environment of deposition.

This Record divides the Carranya Formation into two informal members: a lower tidal mudflats member and an upper tidal sandflats to fluvial member. The lower tidal mudflats member is developed locally at the base of the Carranya Formation and is found at CTS and Bulka east areas (Fig. 11). The upper tidal sandflats to fluvial member characterizes the Carranya Formation at the majority of outcrops, and represents an increase in sediment supply, relative sea-level drop and deposition of a sand-dominated system.

Lower member: tidal mudflats

Macro and trace fossils provide conclusive evidence to support a biologically active shallow-marine environment, while paleocurrents and sedimentary structures indicate a tidally influenced depositional environment. Desiccation cracks observed by McTavish and Legg (1976) near the base of the Carranya Formation at the type section are indicators of subaerial exposure, commonly found in supratidal settings. Flat-topped current ripples (Fig. 9f) are the result of subsequent modification by change in water depth. These ripple types can form in the intertidal zone during falling tides and have been observed forming in very shallow water (<5 cm), where new wave dynamics truncate previously formed ripple crests by erosive conditions (Tanner, 1958). The domination of fine-grained sedimentary rocks in the lower member is also suggestive of a low-energy depositional environment, such as a mudflat in a tidal embayment.

The wide variety of macro and trace fossils suggests a complex and thriving faunal community. Abundant gastropod molds (Fig. 12g), along with rare trilobites and brachiopods (Figs 4 and 12h, respectively) are indicative of a shallow-marine depositional environment for the lower Carranya Formation. Bioturbation also suggests the presence of a diverse range of opportunistic invertebrates, quickly colonizing the sediment–water interface of the intertidal zone before being buried by the next tidal cycle. A succession of shallow- to deep-burrowing organisms can be inferred from the presence of the following trace fossils: *Planolites–Thalassinoides–Chondrites*. This subdivision of feeding tiers suggests rapid depositional rates that are required to preserve nutrients deeper in the sediment that would otherwise be scavenged on the surface (Seilacher, 1967). *Chondrites* in particular, is a burrow with a central shaft from surface that extends below shallow-feeding tiers of deposit-feeding organisms, such as those producing *Planolites* and *Thalassinoides*, and branches out in sediment that has not already been mined of all organic content (Seilacher, 2007).

Upper member: tidal sandflats to fluvial

Distinctive sedimentary structures representative of a sand-dominated, high-energy depositional environment have been observed for the upper member of the Carranya Formation. Characteristics of both tidal sandflats and fluvial environments are present. Erosive sandstone-filled channels (Fig. 8a), repetition of normally graded beds (Fig. 8b), and pebble lags (Fig. 8c) indicate episodic high-energy depositional environments followed by waning flow, consistent with flooding stages in a fluvial system. Pebble lags also represent the thalweg of river channels. Tidal influences in the upper Carranya Formation are indicated with bidirectional paleoflow (Fig. 10), Kinneyia-type wrinkle structures, and the occurrence of a rare gastropod in the upper member (Fig. 11, Log 3B). A number of other sedimentary structures might have resulted from either a tidal sandflat or fluvial depositional environment, including trough cross-bedding (Fig. 9a), tabular intra-formational rip-up clasts (Fig. 8e), slumped bedding (Fig. 8f), and current lineations with crescents (Fig. 9g,h).

Field observations and petrographic evidence from the Carranya Formation indicate a dominance of texturally and mineralogically mature to super-mature quartz arenite based on composition, sorting, and roundness. This type of sandstone is generally the result of a high-energy depositional environment that abrades less stable minerals and winnows out the clay-sized components. Breakdown of minerals is also susceptible to a climate that enables intense weathering. Mature sandstones can also be formed by multiple stages of recycled sedimentary terranes and dissolution of mobile elements during diagenesis. The lack of siltstone and mudstone in this interval may also reflect the lack of land plants at this geological time to assist in preservation, potentially by root binding overbank deposits. The presence of well-rounded, clast-supported, pebble to cobble conglomerate is also consistent with a high-energy fluvial environment.

Provenance

Detrital zircon dating is an important tool in sedimentary provenance studies. The high resistance to abrasion and chemical attack of zircon crystals and the retention of U–Pb isotopic signatures during multiple stages of erosion

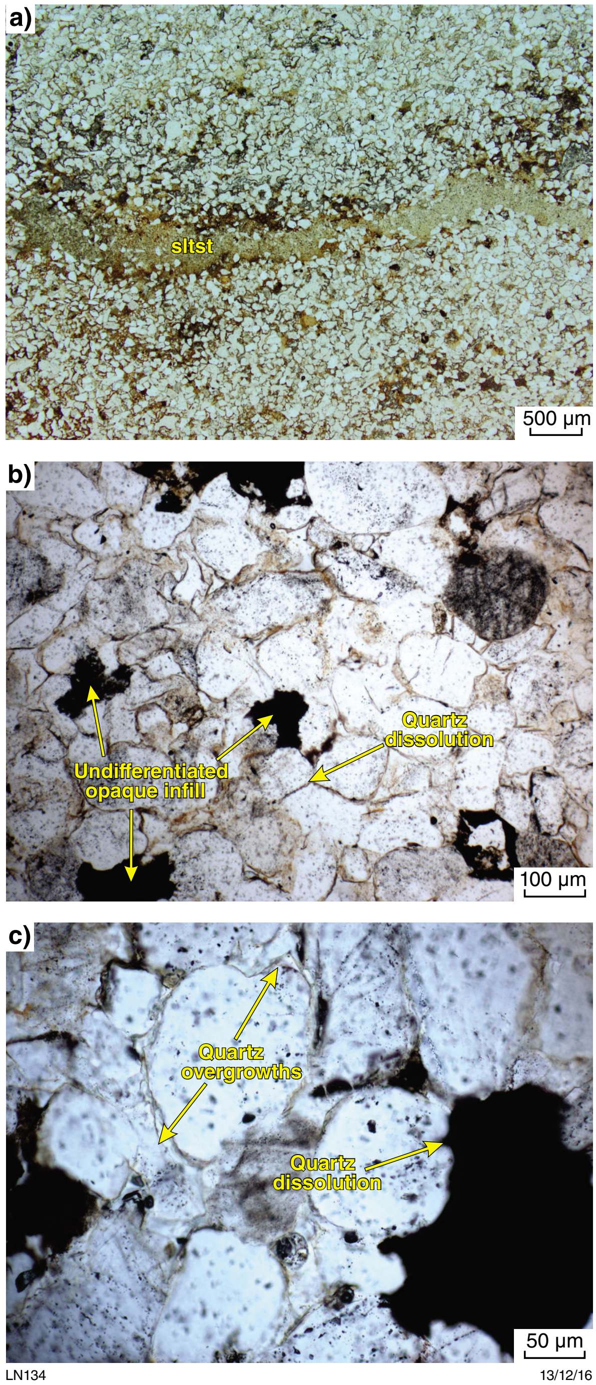

Figure 14. Petrographic images of samples collected from the CTS (WAROX station PWHWCK001, MGA 358267E 7880557N): a) moderate to well-sorted, subrounded to angular quartz arenite with a large, elongate siltstone (sltst) clast in the centre of field of view. Grain sorting indicates textural maturity; angularity of clasts is caused by the growth of sharp crystal faces during quartz precipitation. Reddish-orange iron oxide coatings on the quartz grains provide the colour to the sandstone (TS 135998 PL 10X); b) examples of pressure dissolution around quartz grain boundaries, reprecipitation of optically continuous and euhedral quartz overgrowths and unidentified black pore infill (TS 184269 PL 50 X); c) detailed view of quartz overgrowths, quartz dissolution and unidentified opaque infill of pore space (TS 184269 PL 100X)

and deposition provide a time-scale fingerprint to the original sources of a sedimentary unit (Fedo et al., 2003). A number of studies has focused on the sedimentary provenance of Ordovician strata in the Canning Basin with emphasis on fingerprinting reservoir sandstone (Haines and Wingate, 2007b), links between the Canning and Amadeus Basins (Haines and Wingate, 2007a) and Canning–Officer interbasin connections (Haines et al., 2013).

Detrital zircons analysed from sandstone of the Carranya Formation (MGA 358266E 7880557N; GSWA 184269, Wingate, 2007b) provided a spread of age peaks from the Mesoarchean (3006 ± 8 Ma) to the latest Neoproterozoic (547 ± 7 Ma) (Haines and Wingate, 2007a; Wingate, 2007b; Haines et al., 2013). Up to 19 distinctive age peaks were identified over a time frame of nearly 2.5 billion years (Fig. 15). This illustrates the wide variety of potential sources and the multiple episodes of sediment recycling which culminates in the final deposition of the Carranya Formation.

Even though the detrital zircon signature of the Carranya Formation is complex, a number of significant peaks can be correlated to known primary zircon sources (Haines et al., 2013; Hollis et al., 2014). The earliest peak that can be correlated is at c. 1740 Ma in the late Paleoproterozoic, matching the Aileron Province of the Arunta Orogen to the southeast. A second major peak at c. 1570 Ma correlates to the Paterson Orogen on the opposite side of the Canning Basin to the southwest. A third major peak at 1170 Ma is equivalent to the Musgrave Orogen farther south past the Arunta Orogen. The youngest and perhaps most significant peak within the Carranya Formation detrital zircon spectrum is c. 550 Ma, which may be derived from the 'Pan-Gondwana' source from East Antarctica (Haines et al., 2013). Lesser Paleoproterozoic peaks from the Carranya Formation sample may be sourced from sedimentary units and magmatic events on the North Australian Craton. A peak at c. 1850 Ma falls within the age range of the Lamboo Province (Hollis et al., 2014).

Local correlations using detrital zircon spectra from Ordovician strata in the Canning Basin also provide links between individual sedimentary units. Direct comparisons can be made between detrital zircon spectra of samples from the Wilson Cliffs Sandstone (Wingate and Haines, 2009c), the Goldwyer Formation (Wingate and Haines, 2009b), and the Carranya Formation (Wingate, 2007b) (Fig. 15), all sampled in the eastern part of the basin. They all display a significant late Mesoproterozoic and late Neoproterozoic age component, but vary considerably from the detrital zircon spectrum from the lower Nambeet Formation (Fig. 15; Wingate and Haines, 2009a), sampled from petroleum well Samphire Marsh 1 in the western Canning Basin. A broad correlation based on detrital zircon signatures was also inferred between the source for the Carranya Formation and the Acacia Sandstone Member (Wingate, 2007a) of the Willara Formation, although it should be noted that multiple sources were also acknowledged for the Acacia Sandstone Member (Haines and Wingate, 2007a).

Detrital zircon age analysis and paleocurrent data provide apparently conflicting information regarding the source region for the Carranya Formation. An average paleocurrent flow to the south for the Carranya Formation was first suggested by Haines and Wingate (2007a) based on limited field data. This study has determined a bimodal distribution of paleocurrents based on 23 measurements from four localities (Fig. 10) with a dominant flow to the southeast and weaker flow to the northwest. Taking into account the possibility of some paleocurrent directions originating from tidal flow, a general flow for the depositional system can be taken as the dominant flow to the southeast. This suggests the North Australian Craton to the northwest as the immediate source, contrary to detrital zircon provenance, which indicates a general southerly source with southwest and southeast components. The 'Pan-Gondwana' source, however, is too young to be reworked from Neoproterozoic basins, so at least some of the sediment is derived directly from the south.

A possible explanation for this discrepancy is the partial erosion of a pre-existing Neoproterozoic sedimentary cover over the North Australian Craton, which was originally sourced from a number of Proterozoic provinces to the south or in central Australia. Subsequent uplift of the North Australian Craton eroded the majority of the overlying Neoproterozoic basins that lie north of the Halls Creek Orogen, retaining inliers such as the Louisa Basin (Blake et al., 2000; Hassan, 2000, 2004), including the Mount House Group (Griffin et al., 1993) to the north (Fig. 1). Neoproterozoic basins, such as the Murraba, Wolfe, or Victoria Basins form part of the Centralian Superbasin, which also extends beneath the Canning Basin, based on further detrital evidence (Haines et al., 2013).

Local correlations

Correlation of the Carranya Formation with the lowest siliciclastic succession in the Canning Basin has been previously documented in the literature from both subsurface- and outcrop-based studies (Fig. 2). The suggested correlative intervals include the lower unit of the Wilson Cliffs Sandstone (Playford et al., 1975; McTavish and Legg, 1976), the Nambeet Formation, and Kunian Sandstone (Kennard et al., 1994; Haines and Wingate, 2007a,b). The only potentially age-diagnostic fossil discovered in the Carranya Formation was a single trilobite pygidium, originally identified as *Dikelokephalina* sp. collected at the CTS area (Fig. 4; Gilbert-Tomlinson in Casey and Wells, 1964), which was given an Ordovician age. This fossil specimen was unable to be located in the Geoscience Australia fossil collection and the photo appears to be of a latex mold, which may suggest the fossil was never collected.

Two lines of evidence suggest a possible correlation of the outcropping Carranya Formation with the subsurface Goldwyer Formation. Detrital zircon signatures from the Carranya and Goldwyer Formations have a significant match over the 500 to 1800 Ma range (Fig. 15).

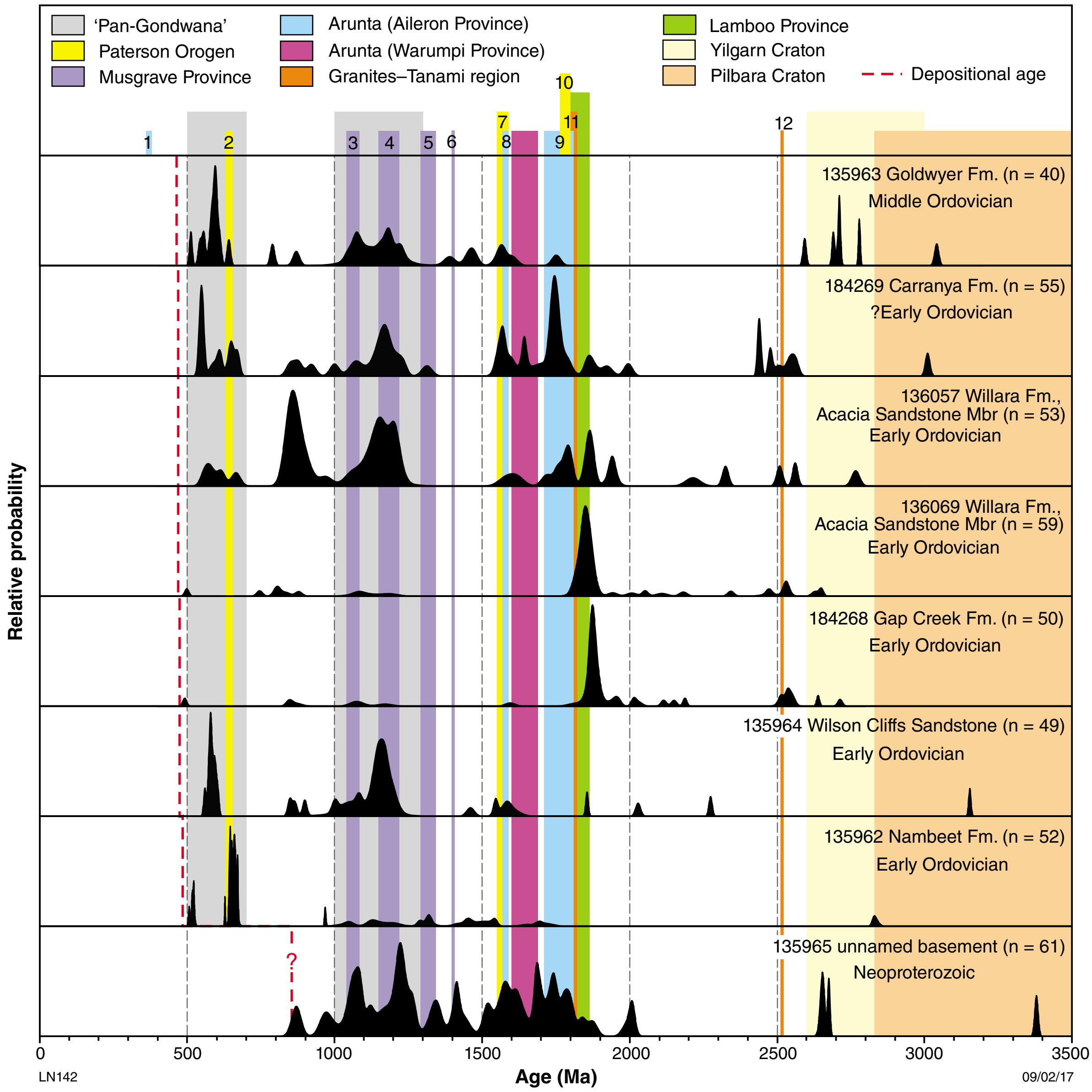

Figure 15. **Stacked probability density plots for Ordovician Canning Basin detrital zircon U–Pb ages. Vertical background bars depict the ages of known potential primary zircon sources (from Haines et al., 2013). Numbers distinguish discrete events or groups of events within terrains: 1 – Alice Springs Orogeny felsic intrusive event; 2 – Miles Orogeny/O'Callaghans Supersuite intrusion; 3 – Giles Event; 4 – Musgrave Orogeny; 5 – Mount West Orogeny; 6 – Papulankutja Supersuite; 7 – Krackatinny Supersuite; 8 – Chewings Orogeny; 9 – Combined Mount Stafford, Yambah, Inkamulla, and Strangways Events; 10 – Yapungku Orogeny; 11 – unnamed igneous event in Granites–Tanami Province; 12 – igneous event recorded in Billabong Complex. Events unlikely to have generated significant volumes of zircon, including mafic igneous events and tectonic events lacking significant magmatic components, are not included.**

Increasing amounts of sand in the Goldwyer Formation from northwest to southeast (Haines, 2004) allow for the correlation of a proximal Carranya Formation to the time-equivalent distal Goldwyer Formation.

The Carranya Formation may be the intermediary formation between the Goldwyer Formation and the coeval Stairway Sandstone in the Amadeus Basin (Jones et al., 1998; Haines, 2004; Haines and Wingate, 2007a). A potential link between the Carranya Formation and the Stairway Sandstone may also provide evidence for the Larapintine Seaway connection between the Canning and Amadeus Basins during the Middle Ordovician, although additional detrital zircon geochronology and biostratigraphic research would be required to make a practical case.

The dominant southeast paleocurrent direction of the Carranya Formation is in disagreement with correlation to a distal Goldwyer Formation to the southwest, as are paleocurrents of the Stairway Sandstone, which flow to the northeast (Haines and Wingate, 2007a).

Hydrocarbon potential

A proximal sandstone dominated equivalent of the Goldwyer Formation along the periphery of the Canning Basin also has inferences on the development of reservoir quality laterally from a known source rock. Sandy intervals in the Goldwyer have generally been restricted to fine-grained facies, which become more prominent in the southeastern portion of the basin (Haines, 2004). Reservoir sandstone units intertonguing with the Goldwyer Formation might provide another petroleum play in the remote eastern edge of the Canning Basin. Such plays could be targeted to the south of the Mueller Fault, where the Ordovician strata have an estimated thickness of 400 m based on seismic. It is important to note, however, that petrographic analysis indicates intergranular porosity has been occluded by the compaction of quartz grains and quartz cementation.

Conclusions

A combination of sedimentology, petrography, ichnology, and detrital zircon geochronology has refined the depositional environment of the Carranya Formation, with implications for provenance, regional correlations, and hydrocarbon potential. Results indicate a lower tidal mudflats member with moderate abundance of both fossil invertebrates and trace fossils, overlain by an upper member, deposited in a tidal sandflats to fluvial setting. This records a relative sea-level drop as a fluvial system progrades into the basin.

Although original source correlations for the Carranya Formation have been made with multiple sources based on detrital zircon geochronology, including the Arunta, Musgrave, and Paterson Orogens and a distal 'Pan-Gondwanan' source, paleocurrents indicate the North Australian Craton as an immediate source to the northwest. The multi-cyclical nature of the Carranya Formation based on the detrital zircon geochronology and petrographic analysis suggests a Neoproterozoic sedimentary cover overlying the North Australian Craton as an intermediate source.

The petrographic evidence that the sandstone is texturally and mineralogically mature to super-mature is likely due to recycling of multiple, pre-existing sandstone units. This is consistent with the detrital zircon evidence for a provenance link between the Carranya Formation and Neoproterozoic basins deposited to the north of the Canning Basin, but originally sourced from the south.

Additional detrital geochronology on adjacent Neoproterozoic basins such as the Wolfe, Murraba, Louisa, and Victoria Basins and further sandstone intervals in the Ordovician succession of the Canning Basin might help define a sequential, provincial source framework for the Centralian Superbasin and the subsequent Paleozoic basins. Sandstone intervals to focus on in the Canning Basin include additional analysis of the Wilson Cliffs Sandstone, Kunian, and Nambeet Formations, and select parts of the Willara and Goldwyer Formations in different parts of the basin.

A weak correlation between the Carranya and Goldwyer Formations is based on comparable detrital zircon signatures in the 500 to 1800 Ma range. The Goldwyer Formation also has a fine-grained sandstone facies, becoming more prominent in the southeastern portion of the basin with the Carranya Formation being a possible lateral transition to the proximal end-member of the Goldwyer Formation. The poor-quality seismic and sparse coverage in this area preclude seismic correlation of these formations.

The Carranya Formation has had limited potential to act as a petroleum reservoir with hydrocarbon charge from source rocks deeper in the basin. Correlation of the Carranya Formation to the Goldwyer Formation could provide lateral depositional change from source to reservoir, providing direct communication of migrating hydrocarbons. Shale intervals of the upper Goldwyer or within the Grant Group might provide a seal where they are laterally extensive.

References

Alpert, SP 1973, *Bergaueria* Prantl (Cambrian and Ordovician), a probable Actinian trace fossil: Journal of Paleontology, v. 47, no. 5, p. 919–924.

Blake, DH, Passmore, VL and Muhling, PC (compilers) 1977a, Billiluna, Western Australia: Geological Survey of Western Australia, 1:250 000 Geological Series Explanatory Notes, 28p.

Blake, DH, Tyler, IM and Page, RW 2000, Regional Geology of the Halls Creek Orogen, *in* Geology and economic potential of the Palaeoproterozoic layered mafic–ultramafic intrusions in the East Kimberley, Western Australia *edited by* DM Hoatson and DH Blake: Australian Geological Survey Organisation, Bulletin 246, p. 35–62.

Blake, DH, Yeates, AN, Passmore, VL, Hodgson, IM, Walton, DG, Muhling, PC and Crowe, RWA (compilers) 1977b, Billiluna, WA Sheet SE52-14 (2nd edition): Geological Survey of Western Australia, 1:250 000 Geological Series.

Brongniart, AT 1828, Histoire des vegetaux fossiles; ou, recherches botaniques et geologiques sur les vegetaux renfermes dans les diverses couches du globe: A Paris, Crochard et Compie, Libraires-Editeurs.

Casey, JN and Wells, AT 1964, The geology of the north-east Canning Basin, Western Australia: Australian Bureau of Mineral Resources, Report 49, 61p.

Cockbain, AE and Hocking, RM 1989, Revised stratigraphic nomenclature in Western Australian Phanerozoic basins: Geological Survey of Western Australia, Record 1989/15, 11p.

Crowe, RWA and Towner, RR 1976, Definitions of some new and revised rock units in the Canning Basin: Geological Survey of Western Australia, Record 1976/24, 22p.

Davies, NS, Liu, AG, Gibling, MR and Miller, RF 2016, Resolving MISS conceptions and misconceptions: a geological approach to sedimentary surface textures generated by microbial and abiotic processes: Earth Science Reviews, v. 154, p. 210–246, doi:10.1016/j.earscirev.2016.01.005.

Eacott, GR, de Souza Kovacs, N and Hollis, JA 2014, Balwina, WA Sheet 4558: Geological Survey of Western Australia, 1:100 000 Geological Series.

Ehrenberg, K 1938, Bauten von Decapoden (*Callianassa* sp.) aus dem Miozän (Burdigal) von Burgschleinitz bei Eggenburg im Gau Nieder-Donau (Niederösterreich): Paläontologische Zeitschrift, v. 20, p. 263–284.

Fedo, CM, Sircombe, KN and Rainbird, RH 2003, Detrital zircon analysis of the sedimentary record: Reviews in Mineralogy and Geochemistry, v. 53, no. 1, p. 277–303, doi:10.2113/0530277.

Griffin, TJ, Tyler, IM and Playford, PE 1993, Record 1992/5, Explanatory notes on the Lennard River 1:250 000 Geological Sheet SE/51-8 Western Australia, Third Edition update: Geological Survey of Western Australia.

Guppy, DJ, Lindner, AW, Rattigan, JH and Casey, JN 1958, The geology of the Fitzroy Basin, Western Australia: Bulletin of the Bureau of Mineral Resources, Australia, no. 36.

Guppy, DJ and Opik, AA 1950, Discovery of Ordovician rocks, Kimberley Division: Australian Journal of Science, v. 12, p. 205–206.

Hagadorn, JW and Bottjer, DJ 1997, Wrinkle structures: Microbially mediated sedimentary structures common in subtidal siliciclastic settings at the Proterozoic–Phanerozoic transtion: Geology, v. 25, no. 11, p. 1047–1050.

Haines, PW 2004, Depositional facies and regional correlations of the Ordovician Goldwyer and Nita Formations, Canning Basin, Western Australia, with implications for petroleum exploration: Geological Survey of Western Australia, Record 2004/7, 45p.

Haines, PW and Wingate, MTD 2007a, Contrasting depositional histories, detrital zircon provenance and hydrocarbon systems: did the Larapintine Seaway link the Canning and Amadeus basins during the Ordovician?, *in* Proceedings of the Central Australian Basins Symposium (CABS) *edited by* TJ Munson, GJ Ambrose and P Ferenczi: Northern Territory Geological Survey; Central Australian Basins Symposium, Alice Springs, Northern Territory, 16 August 2005a; Special Publication 2, p. 36–51.

Haines, PW and Wingate, MTD 2007b, Fingerprinting reservoir sandstone provenance in the Canning Basin using detrital zircons, *in* Geological Survey of Western Australia Annual Review 2005–06: Geological Survey of Western Australia, Perth, Western Australia, p. 59–63.

Haines, PW, Wingate, MTD and Kirkland, CL 2013, Detrital zircon U–Pb ages from the Paleozoic of the Canning and Officer Basins, Western Australia: implications for provenance and interbasin connections, *in* The sedimentary basins of Western Australia IV *edited by* M Keep and SJ Moss: Petroleum Exploration Society of Australia; West Australian Basins Symposium, Perth, Western Australia, 18 August 2013, 19p.

Haines, PW, Wingate, MTD, Kirkland, CL and Allen, HJ 2015, Detrital zircon geochronology of upper Ediacaran to lower Cambrian deposits (Supersequence 4), western Amadeus Basin: testing revised stratigraphic correlations: Geological Survey of Western Australia, Record 2015/8, 35p.

Hassan, LY 2000, Mineral occurrences and exploration potential of the east Kimberley: Geological Survey of Western Australia, Report 74, 83p.

Hassan, LY 2004, Mineral occurrences and exploration potential of the West Kimberley: Geological Survey of Western Australia, Report data package 88.

Hocking, RM 1994, Subdivisions of Western Australian Neoproterozoic and Phanerozoic sedimentary basins: Geological Survey of Western Australia, Record 1994/4, 85p.

Hollis, JA, Kemp, AIS, Tyler, IM, Kirkland, CL, Wingate, MTD, Phillips, C, Sheppard, S, Belousova, E and Greau, Y 2014, Basin formation by orogenic collapse: zircon U–Pb and Lu–Hf isotope evidence from the Kimberley and Speewah Groups, northern Australia: Geological Survey of Western Australia, Report 137, 46p.

Jones, PJ, Nicoll, RS, Edwards, DS, Kennard, JM and Glenn, KC 1998, Canning Basin biozonation and stratigraphy, 1998, *in* Australian Geological Survey Organisation, Chart 2.

Kennard, JM, Jackson, MJ, Romine, KK, Shaw, RD and Southgate, PN 1994, Depositional sequences and associated petroleum systems of the Canning Basin, WA, *in* The sedimentary basins of Western Australia *edited by* PG Purcell and RR Purcell: Petroleum Exploration Society of Australia, Western Australian Branch, Perth, Western Australia, p. 657–676.

McTavish, RA and Legg, DP 1976, The Ordovician of the Canning Basin, Western Australia, *in* The Ordovician system *edited by* MG Bassett: University of Wales Press and National Museum of Wales; Palaeontological Association Symposium, Birmingham, United Kingdom, September 1974; Proceedings, p. 447–478.

Nicholson, HA 1872, Contributions to the study of the errant Annelides of the older Palaeozoic rocks: Proceedings of the Royal Society of London, v. 21, p. 288–290.

Nicoll, RS, Laurie, JR and Roche, MT 1993, Revised stratigraphy of the Ordovician (late Tremadoc–Arenig) Prices Creek Group and Devonian Poulton Formation, Lennard Shelf, Canning Basin, Western Australia: Journal of Australian Geology and Geophysics, v. 14, p. 65–76.

Pickerill, RK and Harris, IM 1979, A reinterpretation of *Astropolithon hindii* Dawson, 1978: Journal of Sedimentary Petrology, v. 49, no. 3, p. 1029–1036.

Playford, PE, Cope, RN, Cockbain, AE, Low, GH and Lowry, DC 1975, The geology of Western Australia (Memoir 2 edition): Geological Survey of Western Australia, Phanerozoic Chapter 2, p. 223–432.

Porada, H and Bouougri, E 2007, 'Wrinkle structures' — a critical review, *in* Atlas of microbial mat features within the clastic record *edited by* J Scheiber, PK Bose, PG Eriksson, S Banerjee, S Sarkar, W Altermann and O Catuneau: Elsevier, p. 135–144.

Salter, JW 1857, On annelide burrows and surface markings from the Cambrian rocks of the Longmynd. No. 2: Quarterly Journal of the Geological Society, v. 13 (199), p. 207, doi:10.1144/GSL.JGS.1857.013.01-02.29.

Seilacher, A 1967, Bathymetry of trace fossils: Marine Geology, v. 5, p. 413–428.

Seilacher, A 2007, Trace fossil analysis: Berlin, Heidelberg, New York: Springer-Verlag, 226p.

Tanner, WF 1958, An occurrence of flat-topped ripple marks (Florida): Journal of Sedimentary Research, v. 28, no. 1, p. 95–96.

Veevers, JJ and Wells, AT 1961, The geology of the Canning Basin: Bureau of Mineral Resources, Geology and Geophysics, Bulletin 60, 323p.

Walcott, CD 1914, Cambrian geology and palaeontology III, no. 2: Precambrian Algonkian algal flora: Smithsonian Miscellaneous Collections 64, p. 77–156.

Wingate, MTD 2007a, 136057: quartz sandstone, Acacia 2; Geochronology Record 655: Geological Survey of Western Australia, 5p.

Wingate, MTD 2007b, 184269: quartz sandstone, Carranya Homestead; Geochronology Record 658: Geological Survey of Western Australia, 5p.

Wingate, MTD and Haines, PW 2009a, 135962: sandstone, Samphire Marsh 1; Geochronology Record 777: Geological Survey of Western Australia, 5p.

Wingate, MTD and Haines, PW 2009b, 135963: sandstone, Wilson Cliffs 1; Geochronology Record 778: Geological Survey of Western Australia, 5p.

Wingate, MTD and Haines, PW 2009c, 135964: sandstone, Wilson Cliffs 1; Geochronology Record 779: Geological Survey of Western Australia, 5p.

Yeates, AN, Crowe, RWA, Towner, RR, Wyborn, AI and Passmore, VL 1975, Notes on the geology of the Gregory Sub-basin and adjacent areas of the Canning Basin, Western Australia: Bureau of Mineral Resources, Geology and Geophysics, Record 1975/77, 268p.

Yeates, AN and Muhling, PC (compilers) 1977, Mount Bannerman, Western Australia (2nd edition): Geological Survey of Western Australia, 1:250 000 Geological Series Explanatory Notes, 24p.

Yeates, AN, Wyborn, LAI, Walton, DG, Crowe, RWA and Muhling, PC (compilers) 1978, Mount Bannerman, WA Sheet SE52-13 (2nd edition): Geological Survey of Western Australia, 1:250 000 Geological Series.

Zhan, Y 2017, Canning coastal seismic survey — a structural overview of the Canning Basin: Geological Survey of Western Australia, Record 2017/5.

This Record is published in digital format (PDF) and is available as a free download from the DMP website at <www.dmp.wa.gov.au/GSWApublications>.

Further details of geological products produced by the Geological Survey of Western Australia can be obtained by contacting:

Information Centre
Department of Mines and Petroleum
100 Plain Street
EAST PERTH WESTERN AUSTRALIA 6004
Phone: +61 8 9222 3459 Fax: +61 8 9222 3444
www.dmp.wa.gov.au/GSWApublications

RECORD 2017/3

PROVENANCE, DEPOSITIONAL SETTING, AND REGIONAL CORRELATIONS OF THE ORDOVICIAN CARRANYA FORMATION, CANNING BASIN

Normore